NASA Technical Memorandum

NASA TM - 108412

AN INVESTIGATION OF SQUEEZE-CAST ALLOY 718

Center Director's Discretionary Fund Final Report
(Project Number 90-10)

By W.R. Gamwell

Materials and Processes Laboratory
Science and Engineering Directorate

June 1993

National Aeronautics and Space Administration

George C. Marshall Space Flight Center

TABLE OF CONTENTS

LIST OF ILLUSTRATIONS

LIST OF TABLES

TECHNICAL MEMORANDUM

AN INVESTIGATION OF SQUEEZE-CAST ALLOY 718

INTRODUCTION

Alloy 718 castings are used extensively as primary structural components in jet and rocket engines; however, their mechanical properties are lower than the wrought alloy. Innovative casting methods are desired which provide increased mechanical properties over those currently available. The squeeze-casting process appears to have potential to obtain mechanical properties (Ftu, Fty, percent E) approaching those of alloy 718 wrought products at reduced cost. If so, squeeze-cast components produced to near net shape can potentially be used as replacements for advanced propulsion system hardware that is normally produced by conventional forging processes.

The space shuttle main engine (SSME) has many structural components made from alloy 718 ring forgings less than 10 inches in outer diameter. The forgings are produced per MIL-F-7190, grade C. They go through an expensive manufacturing cycle to produce finished parts which are used in the SSME low- and high-pressure liquid oxygen (lox) and fuel pumps. Machining costs to produce finished components from ring forgings can represent 80 percent of the total part cost. Near net-shaped, squeeze-cast components are potential low-cost alternatives to ring-forged components in this size range, for use in next-generation propulsion engines. More near net-shaped components may be produced which can substantially reduce overall finished-component manufacturing times and costs.

Squeeze casting is the term used to describe the pressworking of liquid metal into finished shapes.[1 2] Metal is poured into a preheated die cavity which is located on the bed of a hydraulic press. The press closes the die and pressurizes the solidifying metal until solidification is complete. The casting is then ejected from the cavity.

Solidification occurs under pressures up to 60 ksi, which is several orders of magnitude greater than the melt pressure developed in conventional casting practice. Such high pressure levels decrease porosity, keep entrapped gases in solution, and promote contact between the mold and the casting for rapid and more efficient heat extraction. In general, squeeze casting produces a rapidly solidified, pore-free, fine-grained microstructure resulting in mechanical properties that fall midway between conventional casting and wrought products.[1 2]

Squeeze-cast parts do not require runners or gates, and the parts can be made to near net shape with a minimum of materials and near optimum energy utilization. The need for less starting material, lower equipment cost, and minimal machining to configuration contribute to the lower costs of squeeze casting relative to forging. In comparison to conventional castings, any cost increase due to the need for a press is usually more than compensated for by improved material yield (e.g., reduced part rejection and the efficient use of metal) and, more importantly, the higher rate of production made possible by rapid solidification in squeeze casting. This process lends itself to automation, and therefore has excellent potential for producing components with consistently good quality at high production rates.

A preliminary program was conducted at the NASA Marshall Space Flight Center within the Materials and Processes Laboratory to determine the feasibility of squeeze casting superalloys. The current investigation evaluated alloy 718 ring castings of large cross-sectional area produced by the squeeze-cast process.

EXPERIMENTAL PROCEDURES

Alloy 718 ring castings were produced in series for this study. The primary processing parameters that varied were pressure level and duration, with test billets processed at pressures from 42 to 60 ksi for 5 to 90 s. Macrostructural and microstructural characteristics were evaluated, as were mechanical properties.

Materials

This study used alloy 718 produced to conform to AMS 5662E by Inco Alloys International, Inc., under heat number HT3323EY. Composition limits by weight are shown in table 1.

Processing

Ten squeeze castings were made for this study, each approximately 3.0 inches in height with a 2.90-inch inner diameter and a 7.10-inch outer diameter. The squeeze casting billets were produced at the Illinois Institute of Technology Research Institute (IITRI) Surface Engineering Center, Chicago, IL, on a 1,000-ton hydraulic press (fig. 1).

The press was interfaced with a die system used for squeeze casting of the alloy 718 billets. Primary die components for the die system included a punch retaining plate, a punch, a die, a center core, an ejection plate, an ejection shaft, a die spacer plate, and a die stand. Die system components and component materials are listed in figure 2. A conventional die material (IN 100) was used for the die, punch, and ejection plate. Graphite was used for the center core.

The die was protected by a reaction barrier coating. The coating was a yttrium-oxide (Y_2-O_3) base ultra-high temperature refractory paint, spray coated onto the die interior surfaces prior to each pour to enhance die life.

The alloy 718 material was melted in an Al_2-O_3 crucible in a 100-lb induction melting furnace. A lid was placed over the top of the crucible, and an argon gas purge was used as a shield during melting. Melt temperatures were measured using an optical pyrometer. The molten alloy 718 was transferred to the press in a graphite crucible, poured into the metal die, and squeezed.

Processing equipment and materials used to make the squeeze castings are listed in table 2. Standard operating procedures used to make the squeeze castings are provided in table 3. Specific processing parameters used to produce individual billets are shown in table 4. A typical "as-squeeze cast" billet is shown in figure 3.

Billets 2, 4, 5, 6, 9, and 12 were homogenized, and then solution treated and aged (STA). Two homogenization treatments were used on billets 2, 4, 5, and 6. Homogenization treatment A consisted of a 10-h homogenization at 2,075 °F. Homogenization treatment B, used for homogenization of fine-grain alloy 718 castings, consisted of a 36-h homogenization at 2,025 °F.

After homogenization, billet sections were solution heat treated in vacuum at 1,900 °F ±25 °F for 2 h ±15 min, then quickly argon cooled below 1,000 °F. Billet sections were aged at 1,400 °F ±20 °F for 10 h±15 min, furnace cooled to 1,200 °F ±20 °F and held for 10 h ±15 min, and quickly cooled by argon quench to room temperature.

Chemical Composition Analyses

Bulk chemical compositions were determined for billets 1, 2, 4, 5, 6, 9, and 12 using inductively coupled plasma (ICP) and LECO combustion analyses to verify chemistry.

Structural Characterizations

Macrostructural characterizations were performed on billets 1, 2, 4, 5, 6, 9, and 12 in the "as-squeeze cast" condition. Before heat treatment, approximately 1-in-thick plates were removed in a radial direction from each plate. Plate surfaces perpendicular to the radial direction were polished through 0.5-micron alumina and macroetched by Kallings etchant No. 2. Then macrostructural evaluations were performed on these cross sections.

Microstructural characterizations were performed on billets 1, 4, 5, 6, and 12 in the "as-squeeze cast" condition using test specimens from plates that had undergone macrostructural characterization. Plate surfaces perpendicular to the radial direction were polished through 0.5-μm alumina, microetched with Kallings etchant No. 2, and examined with light microscopy.

Microstructural characterizations were performed on billets 2, 4, 5, 6, 9, and 12 after homogenization and STA. Electron microprobe analyses were performed throughout cross sections of billet 12 in the "as-squeeze cast" and heat-treated conditions for phase identification purposes.

Mechanical Properties

Ultimate tensile strength, yield strength, percent elongation, and percent reduction in area were determined in the longitudinal direction for billets 2, 4, 5, 6, 9, and 12 in the heat-treated condition.

Tensile specimens were taken from locations away from areas that contained hot cracking and macroshrinkage effects. In billets 2 and 5, tensile specimens were extracted within 1.5 in from the outer diameter surfaces, proceeding around their circumferences. In billets 4, 6, 9, and 12, tensile specimens were taken throughout billet cross-sectional areas, proceeding around the circumference.

Tensile testing was conducted at room temperature, using a model 880 material test system (MTS) with a 20-kip load frame, in accordance with American Society for Testing Materials (ASTM) E8 procedures. Smooth tensile specimen configurations for the mechanical property testing are shown in figure 4.

Fractography

Fractured tensile specimens taken from billets 2, 4, 5, 6, and 9 were examined with a stereomicroscope at magnifications from × 10 to × 35. A scanning electron microscope (SEM) was used to perform fractography on fracture surfaces from billet 12.

RESULTS

Chemical Compositions

Chemical compositions for the AMS 5662E bar stock used for melting and for billets 1, 2, 4, 5, 6, 9, and 12 are shown in table 5.

"As-Squeeze" Cast Macrostructures

Macrostructures of billet 1, 2, 4, 5, 6, 9, and 12 cross sections representative of specific processing parameters are shown in figures 5 through 11. The macrostructures were taken at × 2 to × 3 magnification.

Billet 1 did not etch very well and did not reveal a very good macrostructure. This billet shows significant areas of macroshrinkage within its interior (fig. 5). This billet was poured short (i.e., it was shorter than the other billets).

Billet 2 contained regions of macroshrinkage in the center-to-lower sections, hot tears in the center-to-upper-right-hand section, columnar grains along the top edge, and equiaxed grains of various sizes throughout the rest of the cross section (fig. 6). Billet 2 contained curved inner diameter surfaces caused by core erosion (see Discussion).

Billet 4 showed an indistinct macrostructure that contained small equiaxed grains (fig. 7). The black linear features were thick and thin bands of Laves phase, which resulted from macrosegregation during solidification. Brown stains on the macrograph were the result of etching porous regions of the cross section.

Billet 5 showed an indistinct macrostructure, with a large region of macroshrinkage and some hot tearing in the center interior (fig. 8). Fine equiaxed grains of various sizes comprised most of the cross section, and curved inner diameter surfaces occurred.

Billet 6 showed an indistinct macrostructure that contained small equiaxed grains, along with a small region of macroshrinkage in the interior (fig. 9). As in billet 4, Laves phase bands and etching stains were seen.

Billet 9 showed a macrostructure similar to those seen in billets 4 and 6, including indistinct areas of small equiaxed grains and Laves phase bands (fig. 10). Curved inner diameter surfaces also occurred.

Billet 12 showed a classic casting macrostructure including the outer chill zone, the intermediate columnar zone, and the central equiaxed zone (fig. 11). This billet contained curved inner diameter surfaces. However, no indications of shrinkage or porosity were seen, and significant structural refinement was noted in the lower left and right sections.

"As-Squeeze" Cast Microstructures

Microstructures exhibited within various areas of "as-squeeze cast" billets 1, 4, 5, 6, and 12 representative of specific processing parameters are shown in figures 12 through 16. Microstructures were taken from the previously macroetched billet cross sections.

Billet 1 showed an unusual microstructure for alloy 718 (fig. 12). Five distinct phases or features can be seen within the microstructure: a matrix phase, a black phase, two lath plate-like phases (only distinguishable visually by color), and a fine phase growing along crystallographic planes. This complex microstructure is believed to be the result of slow cooling. The die system punch has a stop which allows only limited squeezing action on the melt. As reported previously, billet 1 was poured short. Hence, it is believed that the desired pressure was not achieved, slow cooling of the billet occurred, and the observed microstructure resulted.

Billet 4 showed varying microstructures, depending upon location within the billet (fig. 13). Section 4*a* showed typical dendritic microstructural features (with matrix and Laves phase) representative of "as-cast" alloy 718, as well as an atypical banded Laves phase. Section 4*b* showed a dendritic structure without a Laves phase. Section 4*c* showed a semidendritic/semifine equiaxed grain structure with minimal Laves phase. Section 4*d* showed a semidendritic structure with black linear features interspersed throughout the area. Laves phase is contained within the interdendritic regions. It appeared that the interdendritic regions and Laves phase were being suppressed (e.g., squeezed out) by the action of pressure on the solidifying structure and that grain boundaries form at prior interdendritic regions. The black linear features were etch effects due to segregation within the solidifying structure.

Billet 5, sections *a* to *d*, showed equiaxed grains of various sizes throughout the billet cross section (fig. 14). The dark regions were again preferentially etched features, which reflect light poorly.

Billet 6 contained varying microstructures dependent upon location within the billet. Section 6*a* contained typical dendritic features (with matrix and Laves phase) representative of phases existing in conventionally cast alloy 718, as well as the banded Laves phase. Section 6*b* showed a dendritic structure with some black linear features indicating segregation and some faint grain boundaries/grains. Sections 6*c* and 6*d* showed fine equiaxed grains, some banding of Laves phase, with residual dendritic structural patterns and Laves phase banding.

Billet 12, sections *a* to *c*, showed typical dendritic microstructural features (with matrix and Laves phase) representative of phases existing in conventionally cast alloy 718 (fig. 16). Section 12*d* showed fine equiaxed grains with some residual Laves phase and dendritic structural patterns. The grains were approximately eight times smaller than grains from conventionally cast alloy 718.

Heat-Treated Microstructures

Microstructural characterization was performed on billets 2, 4, 5, 6, 9, and 12 after homogenization and STA. Representative longitudinal sections were examined adjacent (e.g., within 1/2 in) to fracture surfaces of mechanically tested tensile specimens.

Heat-treated specimens from billets 2, 4, 5, 6, and 9 had the same microstructural phases seen in heat-treated conventional castings, including complete elimination of the "as-squeeze cast" dendritic pattern (fig. 17). The microstructures contained matrix, niobium carbides (light phase), and a small amount of titanium nitrides (square and triangular phases). However, various morphologies and particle size distributions were seen throughout the niobium carbide and titanium nitride phases, and the phases themselves were nonuniformly distributed throughout cross sections. Heat treatment did not have an effect on macrostructural defects such as shrinkage and hot cracking, and they were not eliminated within these billets.

Billet 12 had the best "as-squeeze cast" macrostructural and microstructural features, as well as the best combination of mechanical properties after heat treating. Heat treated microstructures were typical of those for conventionally cast plus heat-treated alloy 718. The "as-squeeze cast" dendritic pattern had been completely eliminated by the heat treatment. The microstructure contained the expected matrix, niobium carbides (light phase), and a small amount of titanium nitrides (dark phase at × 1,000). Optical and SEM microstructures characteristic of heat-treated tensile specimens are shown in figure 18.

Mechanical Properties

Mechanical properties for billet 12 are shown in table 6. Mechanical properties for billets 2, 4, 5, 6, and 9 are shown in the appendix (tables A1 to A5). Table headings indicate homogenization treatments (A or B) received by each billet. Mechanically tested tensile specimens for billets 2, 4, 5, 6, and 9 are shown in the appendix (figs. A1 to A3).

Fractography

Fracture surfaces from mechanically tested tensile specimens representative of each billet are shown in the appendix (figs. A4 to A6). For each tensile specimen from billets 2, 4, 5, 6, and 9, the fracture surface was examined with a stereomicroscope at magnifications from × 8 to × 35. Observations for each tensile specimen are noted in tables A1 to A5. SEM fractographs showing a typical fracture surface from a billet 12 tensile specimen at × 100 and × 1,000 are shown in the appendix (fig. A6).

DISCUSSION

Macro and Microstructural Features

"As-squeeze cast" billets exhibited a wide range of macrostructural and microstructural features which resulted from the solidification process. During casting, solidification occurs by the nucleation of small grains which grow under the influence of the prevailing crystallographic and thermal conditions

within a system. The size and character of these grains (e.g., equiaxed, columnar) are controlled by the composition of the alloy and by cooling rates.[3–5]

As a casting solidifies, three major factors must be considered: growth of the solid grains, heat evolution and transfer, and dimensional changes (shrinkage), although many other variables also affect the process.[3] The macroscopic structure of an as-cast ingot depends on the rate of nucleation and the rate of heat removal from the casting.[4]

Columnar grains in billets 2 and 12 formed as a result of constitutional supercooling, a condition in which the liquid just in front of a solidifying front is at a temperature below its equilibrium liquidus temperature (e.g., the liquid is supercooled). "Constitutional" indicates that the supercooling arises from a change in composition, not temperature. This condition promotes the growth of solid perturbations into the liquid in a direction opposite that of heat flow and laterally, as well, resulting in a dendritic structure.[3 5]

Equiaxed grains in billet 12 and upper-central portions of billet 2 formed because the temperature in the center of the casting dropped low enough for nucleation to occur before the columnar grains could reach it. These grains were more equiaxed in shape, due to isotropic heat removal from billet centers.[3 4]

Relatively fine-grained structures are possible by promoting constitutional supercooling in conjunction with the use of nucleating agents (e.g., inoculants) to promote heterogeneous nucleation and the absence of thermal gradients (e.g., heat removed isotropically) within the solidifying liquid.[3–5] Additionally, pressure pulses of sufficient intensity have been shown to cause heterogeneous nucleation in undercooled billets, promoting formation of fine-grained structures as well.[5] If cooling rates result in a condition in which the liquid at the solidifying front is highly supercooled, the temperature differential (delta T) below the equilibrium liquidus temperature may be low enough to promote random nucleation and the formation of equiaxed grains.[5]

Fine-equiaxed grains in billets 4, 5, 6, and 9 and the lower portions of billet 2 probably resulted from constitutional supercooling and some combination of heterogeneous nucleation, fast isotropic heat removal, and pressure pulses within the solidifying billets. Columnar grain growth was believed to be inhibited due to compositional and thermal adjustments, and equiaxed grain growth was promoted by a combination of the factors previously mentioned.

Shrinkage

Macroshrinkage consists of isolated, clustered, or interconnected voids in a casting that are detectable macroscopically. This condition is caused by insufficient feeding of liquid metal to compensate for solidification shrinkage.[1] Macroshrinkage exhibited in billets 1, 2, 5, and 6 was probably caused by insufficient pressure during squeezing to compensate for solidification shrinkage and/or from premature release of pressure during processing.

Segregation

Macrosegregation was exhibited in billets 1, 2, 4, 5, 6, and 9. Segregation is a casting defect involving a concentration of alloying elements at specific regions. Macrosegregation refers to gross differences in concentration from one area of a casting to another and is caused by the movement of

liquid or solid within the mushy zone, the chemical composition of which is different from the mean composition. Many driving forces exist for this liquid or solid movement.[15] The macrosegregation seen in billets 2, 4, 5, 6, and 9 probably resulted from a combination of capillary force, solidification shrinkage, thermal contractions, density differences caused by phase of compositional variations, and applied external pressure.

Hot Cracks

Billets 2, 5, and 9 exhibited hot cracking, which may form in cast metal after solidification and during cooling.[1] During billet processing, applied external pressure was quickly released and the castings began to cool. This condition promoted simultaneous expansion and contraction within the billets, creating the internal stresses necessary to produce hot cracking. The elimination of hot cracking should be possible by increasing the hold time of applied pressure on the castings.

Billet Inner Diameter Curved Surfaces

Billets 2, 5, 9, and 12 exhibited inner diameter curved surfaces, which resulted from a fracture of the graphite core. Cores were shaped like an inverted tee, with a 90° corner that had no radius on the fillet area between the core head and shank (fig. 2). These billet cores failed at the fillet area, resulting in the curved inner diameter surfaces noted. The billets showed that the shank portion of the tee had an opportunity to float up after fracture. Concurrently, the downward action of the punch limited the amount of core lateral and upward movement. The cores probably failed during die filling as a result of thermal shock acting on the sharp notch at the core fillet areas.

Processing Parameter/Structure Correlation

Squeeze-cast process variables include melt volume, pouring temperature, tooling temperatures (e.g., die, punch, and core), tooling lubrication/thermal barrier coating, time delay during die closing and pressure application, pressure level, and pressure duration.[12] Optimization of these squeeze-cast processing parameters is critical to the quality and reproducibility of squeeze-cast components, and they must be optimized for each component geometry. Failure to do so can result in defects such as oxide inclusions, porosity, extrusion segregation, blistering, underfill, cold laps, hot cracking or tearing, sticking, case bonding, and extrusion bonding.[12]

Process optimization was not the overriding goal of this investigation. The squeeze casting of alloy 718 was investigated to determine the feasibility of squeeze casting superalloys, regimes of acceptable processing parameters, and primary processing parameter/structure/mechanical property relationships for the subject billet geometry.

During this investigation, the primary processing parameters that were varied were pressure level and pressure duration. No experience base exists on the squeeze casting of superalloys. Appropriate squeeze-cast processing parameters were not known prior to this investigation. Based on the squeeze casting of stainless steel, it was expected that pressure levels greater than 20 ksi and time delays around 30 s were expected to produce acceptable castings.

Due to program constraints, the 10 squeeze castings were produced in series without any intermediate structural or mechanical property evaluation. Processing parameters were selected at the beginning of the program and did not change during the work. As such, no processing parameter optimization was conducted.

Process parameter/structure/mechanical property trends resulting from the combination of pressure levels and durations used in this investigation are not apparent. However, some observations are reported:

- Processing parameter combinations used in this investigation produced casting defects (e.g., shrinkage, extrusion segregation, hot cracks, and underfill) known to be associated with the squeeze-casting process.

- Pressure levels from 42 to 60 ksi were used. Billets 2, 4, 5, 6, and 9 squeezed with high pressure levels from 42 to 51 ksi showed relatively poor structures and mechanical properties. Billet 12 squeezed with the highest pressure level of 60 ksi showed good structure and mechanical properties. Pressure level alone does not appear to be sufficient to obtain sound, defect-free squeeze castings. However, combinations of pressure level (20 to 40 ksi) and pressure duration (60 to 120 s) should be tested to verify this expectation.

- Pressure durations from 5 to 90 s were used. With pressure durations of 35 s or less, billets 2, 4, 5, 6, and 9 showed relatively poor structures and mechanical properties. Billet 12, with a pressure duration of 90 s, showed a relatively good structure and mechanical properties. Pressure duration is expected to play an important role in obtaining sound, defect-free squeeze castings. Casting not held under pressure long enough is expected to be prone to macroshrinkage, hot cracking, and undesirable microstructural features.

Proper combinations of pressure level plus pressure duration are necessary to obtain sound, defect-free squeeze castings of the subject billet geometry. Based on the results of this investigation, pressure durations greater than 35 s are required. It is uncertain whether lower pressure and longer pressure duration combinations will produce sound castings. Further work is recommended to investigate a range of pressure levels with higher pressure durations.

Mechanical Properties

Billet 12 shows the best overall combination of mechanical properties, with an ultimate tensile strength greater than 80 percent of wrought alloy 718 bar. The mechanical properties did vary depending upon location within the billet. The mechanical properties of wrought, squeeze-cast billet 12, and conventionally cast alloy 718 are compared as a percentage of wrought properties in table 7. The percent elongation for squeeze-cast billet 12 is shown to be lower than that for conventionally cast alloy 718, based on property variation within the billet. Higher elongations are expected with squeeze-cast process optimization.

The improved mechanical properties of billet 12 are attributed to its classical macrostructure, a refined microstructure (e.g., smaller grain size than conventional castings), and reduced porosity within the casting as a result of applied pressure during solidification. Mechanical properties were not as good and were highly variable for billets 2, 4, 5, 6, and 9 (see the appendix). These billets showed property variations attributed to a wide range of macrostructural and microstructural features in the "as-squeeze

cast" condition (such as shrinkage, segregation, hot tears, different grain sizes, and columnar and equiaxed grains). Optimization of the process parameters should eliminate these defects and improve the mechanical properties.

CONCLUSIONS

1. This investigation confirms the feasibility of squeeze casting of alloy 718, with promising results.

   (a) The squeeze-cast process can produce large castings of relatively simple shape with refined microstructures free of macroshrinkage, hot tears, and macrosegregation, with mechanical properties approaching those of wrought alloy 718 bar (e.g., yield and ultimate tensile strength at 80 to 90 percent of that of the wrought alloy—billet 12).

   (b) The improved properties appear to be the result of improvements in structure (attributed to grain refinement and reduced porosity).

2. A wide variety of macrostructures and microstructures are produced, dependent upon the squeeze-cast processing parameters.

3. Mechanical properties exhibited in these squeeze-cast alloy 718 billets were highly sensitive to processing parameters. The best billet was obtained at high pressure (60 ksi) with a long holding time (90 s).

4. Process optimization is expected to further improve structural and mechanical properties.

REFERENCES

1. "ASM Metals Handbooks," Ninth Edition, vol. 15, Castings, 1988.

2. Dorsic, J.L., and Verma, S.K.: "Squeezing Production Costs From Metal-Ceramic Composites." Metals Progress, May 1988.

3. Heine, R.W., Loper, C.R., Jr., and Rosenthal, P.C.: "Principles of Metal Casting." McGraw-Hill, 1967.

4. Barrett, C.R., Nix, W.D., and Tetelman, A.S.: "The Principles of Engineering Materials." Prentice-Hall, 1973

5. Flemings, M.C.: "Solidification Processing." McGraw-Hill, 1974.

Table 1. AMS 5662E composition (percentages by weight).

	Minimum	Maximum
Carbon	—	0.08
Manganese	—	0.35
Silicon	—	0.35
Phosphorus	—	0.015
Sulfur	—	0.015
Chromium	17.00	21.00
Nickel	50.00	55.00
Molybdenum	2.80	3.3
Columbium + tantalum	4.75	5.5
Titanium	0.65	1.15
Aluminum	0.20	0.80
Cobalt	—	1.00 max
Boron	—	0.006
Copper	—	0.30
Lead	—	0.0005 (5 p/m)
Bismuth	—	0.00003 (0.3 p/m)
Selenium	—	0.0003 (3 p/m)
Iron	Remainder	

Table 2. System/equipment and materials.

• 1,000-ton press for squeeze casting	(IITRI owned)
• Die system components	
• Punch retaining plate	(Steel)
• Punch	(IN 100)
• Die	(IN 100)
• Center core	(Graphite)
• Ejection plate	(IN 100)
• Ejection shaft	(H13 tool steel)
• Die spacer plate	(IITRI owned)
• Die stand	(IITRI owned)
• Die thermal barrier coating	(Y_2-O_3 based)
• 100-lb induction melting furnace	(Al_2-O_3 crucible)
• Transfer crucible	(Graphite)
• Billet material	(Alloy 718)

Table 3. Standard procedures for squeeze casting alloy 718 billets.

1. Coat die with thermal barrier coating.
2. Set press speed and load level.
3. Heat die by induction to 700 °F.
4. Melt the alloy; superheat between 2,500 to 2,900 °F.
5. Heat graphite transfer crucible to 600 °F.
6. Heat graphite center core to 600 °F.
7. Insert graphite core into die.
8. Transfer molten alloy 718 to graphite crucible.
9. Pour molten alloy into die.
10. Close die, pressurize, and hold for desired time.
11. Release pressure and open die, measure casting temperature.
12. Eject casting from die.
13. Inspect and label casting.
14. Inspect die.
15. Repeat process

Table 4. Process parameters used for squeeze cast alloy 718 billets.

Billet Number	Punch Temperature (°F)	Die Temperature (°F)	Time Delay (s)	Pressure (ksi)	Pressure Duration (s)	Melt Temperature (°F)	Pouring Temperature (°F)	Billet Temperature (°F)
1	700	700	18	53	10	2,642	2,400	2,100
2	670	700	20	51	5	2,600	2,400	2,140
4	650	700	15	51	15	2,596	2,400	2,110
5	600	700	20	42	20	2,600	2,500	2,100
6	600	700	15	54	20	2,642	2,500	2,000
7	650	600	15	48	30	2,640	2,400	2,100
8	650	700	20	48	30	2,642	2,400	2,010
9	710	600	15	48	35	2,642	2,550	2,100
10	700	700	15	48	15	2,642	2,500	2,100
12	700	700	15	60	90	2,850	2,500	2,000

Table 5. Billet/raw material chemical compositions.

Element	AMS 5562E (wt.%)	Billet 12 (wt.%)	Billet 9 (wt.%)	Billet 6 (wt.%)	Billet 5 (wt.%)	Billet 4 (wt.%)	Billet 2 (wt.%)	Billet 1 (wt.%)	Melt Stock (wt.%)
Ni	50–55.00	52.63	53.69	53.34	54.75	53.47	54.15	52.24	53.30
Fe	Balance	Balance	Balance	18.41	Balance	18.50	Balance	18.44	18.56
Cr	17–21.00	18.54	19.17	17.78	19.02	17.84	17.22	16.13	18.15
Cb+Ta	4.75–5.5	4.94	5.31	5.31	4.87	5.20	4.20	3.72	5.13
Mo	2.8–3.30	2.81	3.29	3.16	2.88	3.15	2.80	2.97	2.92
Ti	0.65–1.15	0.83	1.01	0.90	0.87	0.92	0.90	0.15	0.94
Al	0.20–0.80	0.45	0.55	0.48	0.58	0.45	0.53	1.33	0.58
Co	1.00 max	0.090	0.100	0.010	NAF	0.020	0.100	0.010	0.08
Si	0.35 max	0.070	ND	0.330	NAF	0.200	ND	3.090	0.12
Mn	0.35 max	0.080	0.110	0.050	NAF	0.050	0.100	0.040	0.10
Cu	0.10 max	0.100	0.050	0.060	NAF	0.060	0.100	0.070	0.08
C	0.08 max	0.044	0.032	0.034	0.034	0.033	0.030	1.600	0.03
S	0.015 max	0.003	0.003	0.002	0.005	0.002	ND	0.004	0.001
P	0.015 max	0.006	0.006	0.009	NAF	0.010	0.002	0.006	0.010
B	0.006 max	0.003	0.003	ND	NAF	ND	0.002	ND	0.002

Table 6. Mechanical properties for billet 12A.

Longitudinal Tensile Specimens

Specimen Number	Specimen ID	Orientation	Ftu (ksi)	Fty (ksi)	Percent Elongation	Percent RA
1	12-1	L	164.7	146.6	—	15.0
2	12-2	L	164.0	143.6	9.0	36.7
3	12-3	L	162.9	143.0	10.5	25.1
4	12-4	L	160.4	143.5	8.6	8.5
5	12-5	L	156.3	134.4	6.8	14.5
6	12-6	L	163.5	140.0	5.1	7.5
7	12-7	L	166.4	143.8	2.9	4.9
8	12-8	L	165.2	140.1	9.0	25.9
9	12-9	L	167.9	145.0	3.5	13.9
10	12-10	L	154.3	137.3	3.9	16.0
11	12-11	L	168.6	—	—	—

Table 7. Comparison of mechanical properties of wrought, billet 12, and conventionally cast alloy 718 as a percentage of wrought properties.

	Percent of Wrought Property			Relative Ranking
	Ftu	Fty	%E	Average Grain Diameter
Wrought	1	1	1	1 (ASTM No. 5)
Billet 12	0.81	0.90	0.46	11 times larger
Conventionally cast	0.70	0.70	0.65	82 times larger

Notes:

1. Ftu = ultimate tensile strength
2. Fty = yield strength
3. Typical properties for AMS 5662E wrought bar; Ftu = 200 ksi, Fty = 160 ksi, %E = 12%.
4. Typical properties for AMS 5383 investment casting; Ftu = 125 ksi, Fty = 110 ksi, %E = 5%.
5. Expected minimum properties for critical grade castings; Ftu = 140 ksi, Fty = 120 ksi, %E = 6%.

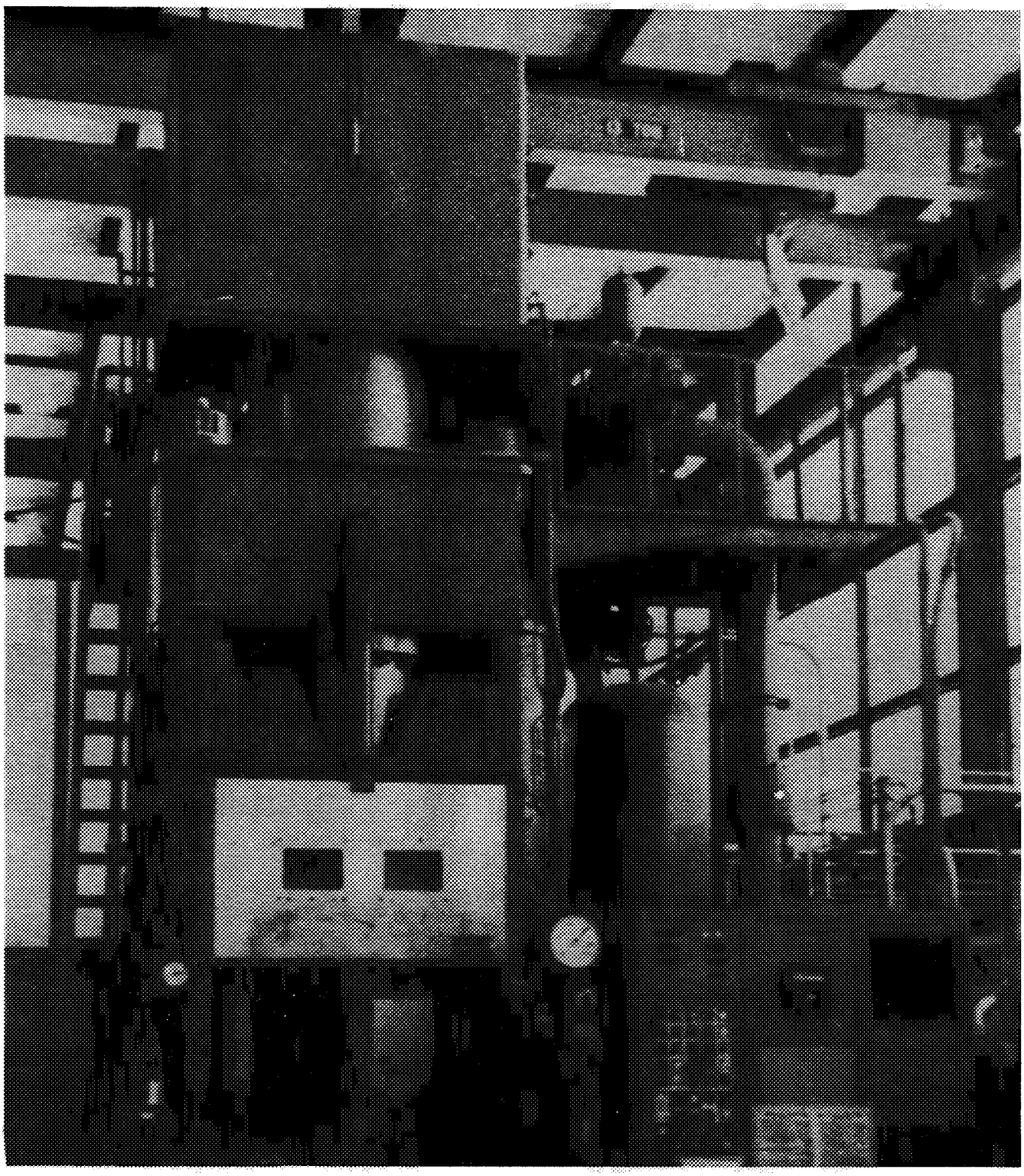

Figure 1. One-thousand-ton hydraulic press used to make the squeeze castings.

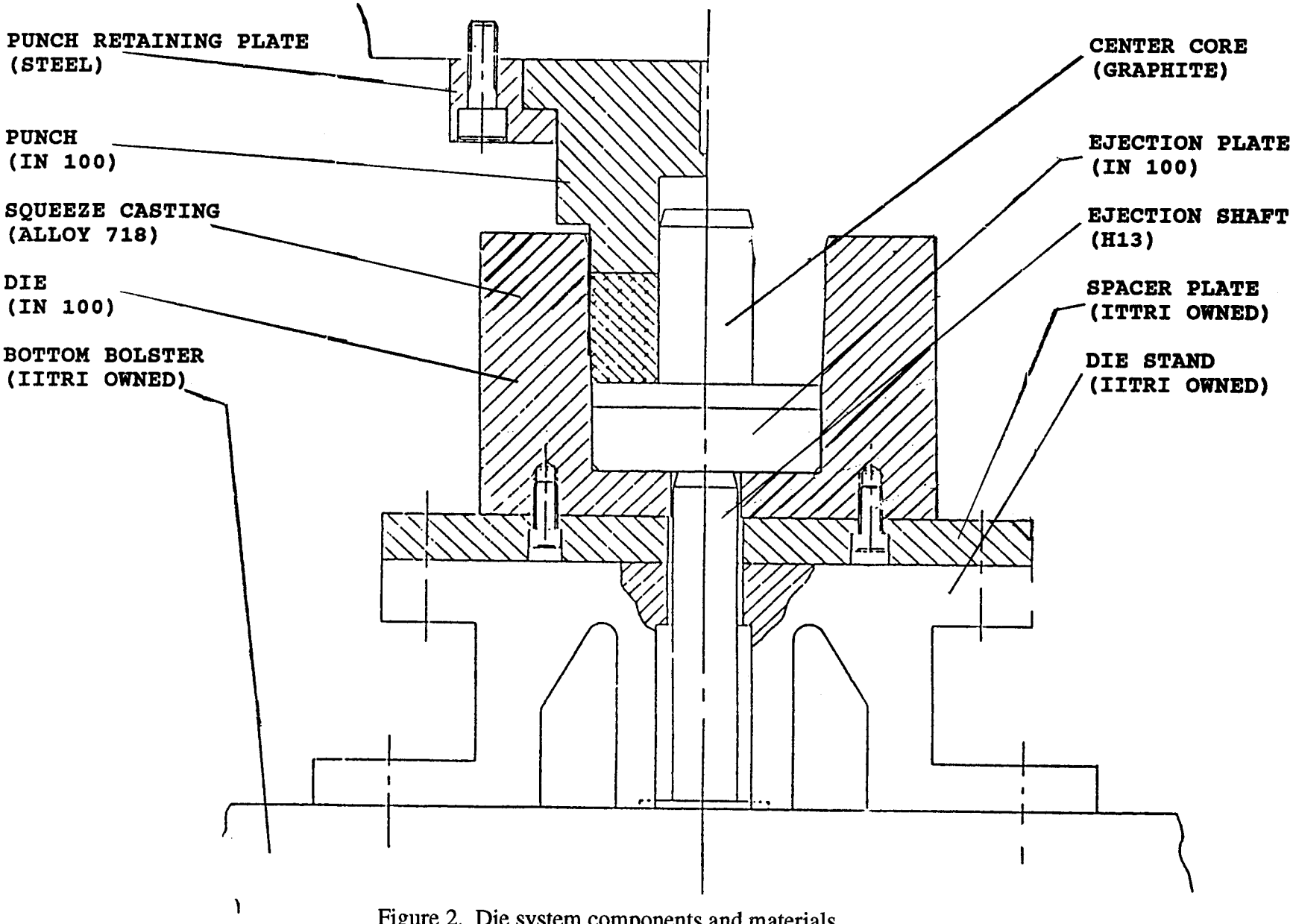

Figure 2. Die system components and materials.

Figure 3. Typical squeeze-cast billet post processing.

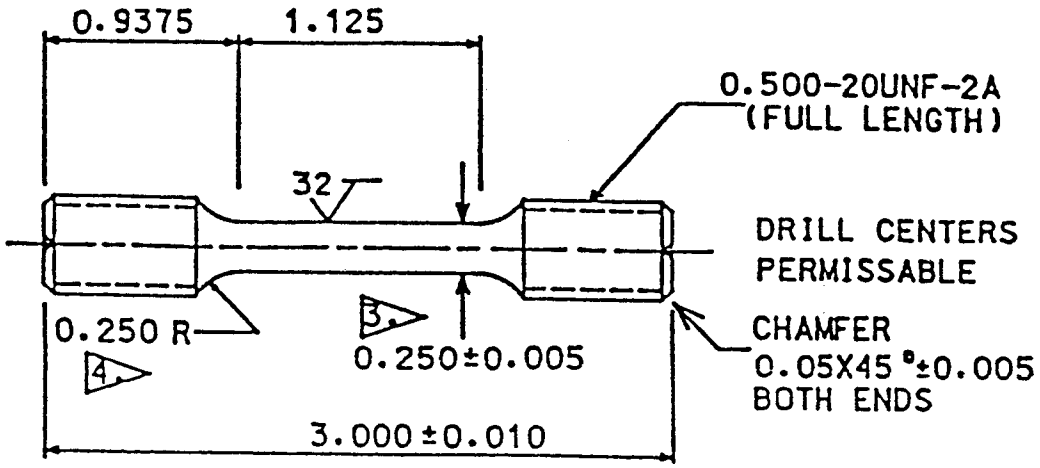

NOTES:

1. ALL DIAMETERS CONCENTRIC WITHIN 0.005 TIR
2. ALL DIMENSIONS IN INCHES
3. SLIGHT TAPER TO CENTER REQUIRED (0.002 MAX)
4. DO NOT UNDERCUT RADII
5. NOT TO SCALE, WORK TO DIMENSIONS GIVEN
6. UNSPECIFIED TOLERANCES ± 0.005 INCHES

Figure 4. Smooth tensile specimen configuration for mechanical property tests.

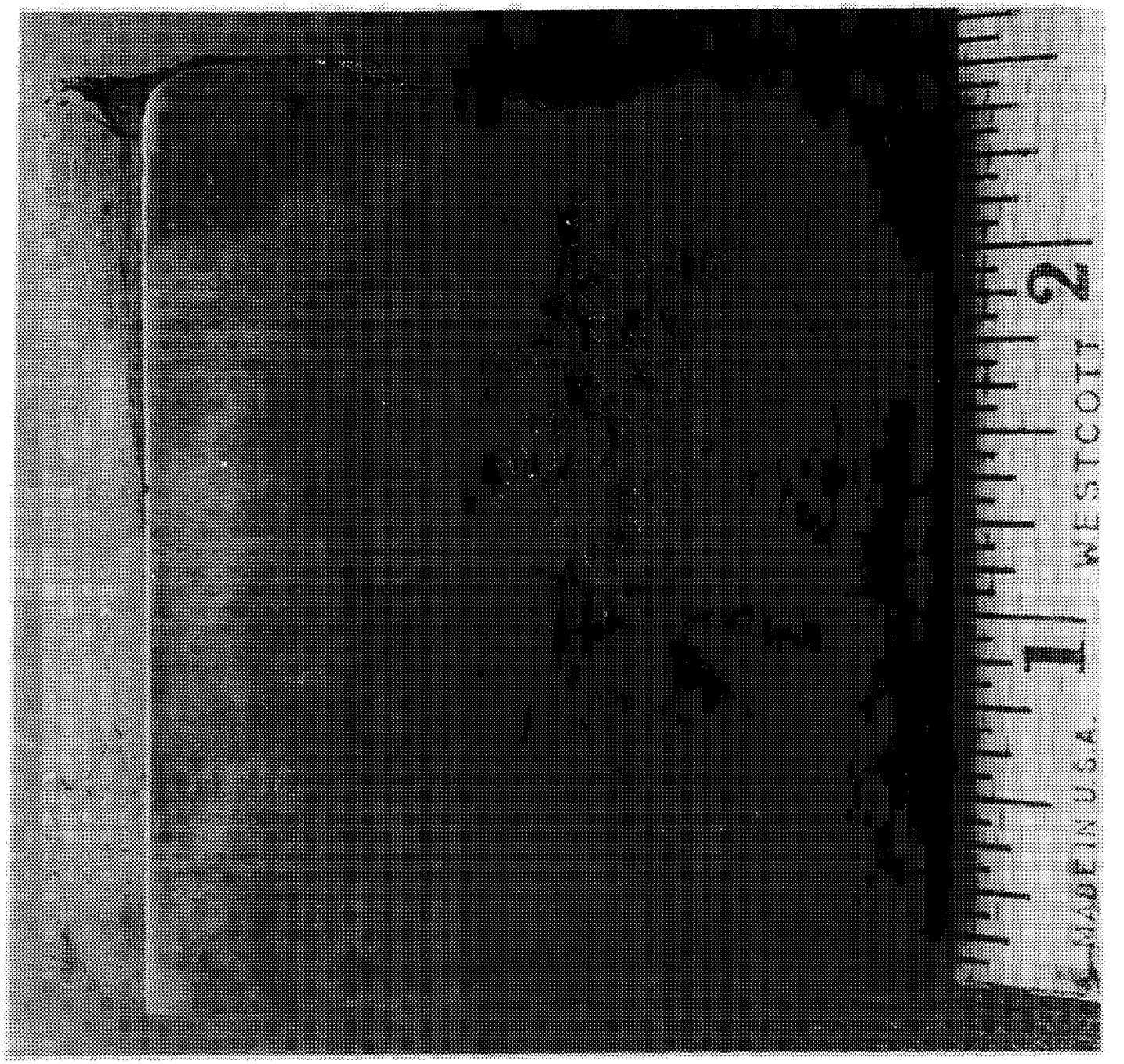

Magnification × 2.4 Etchant: Kallings reagent No. 2

Figure 5. As-squeeze cast macrostructure of billet 1.

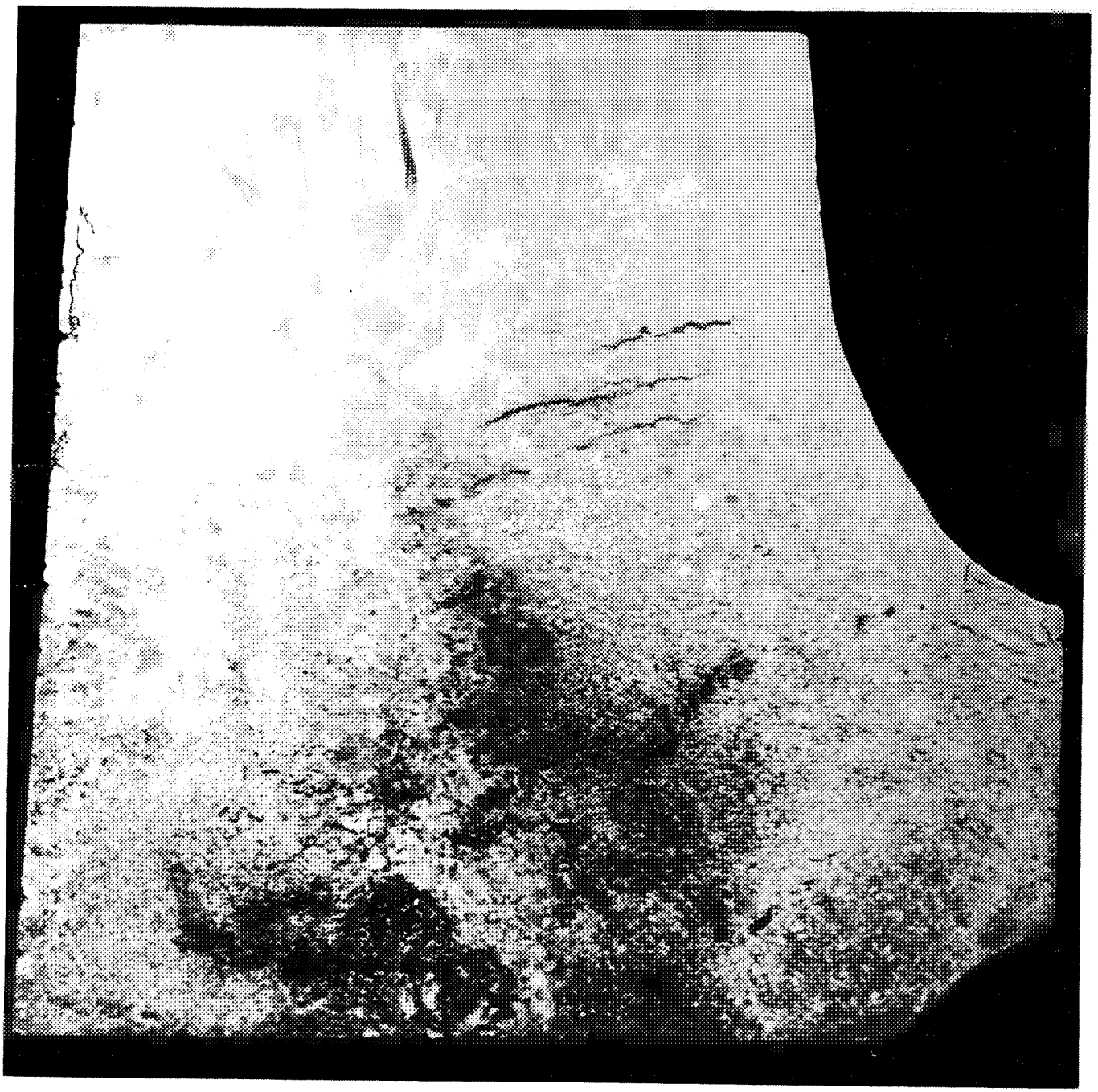

Magnification × 2.2

Etchant: Kallings reagent No. 2

Figure 6. As-squeeze cast macrostructure of billet 2.

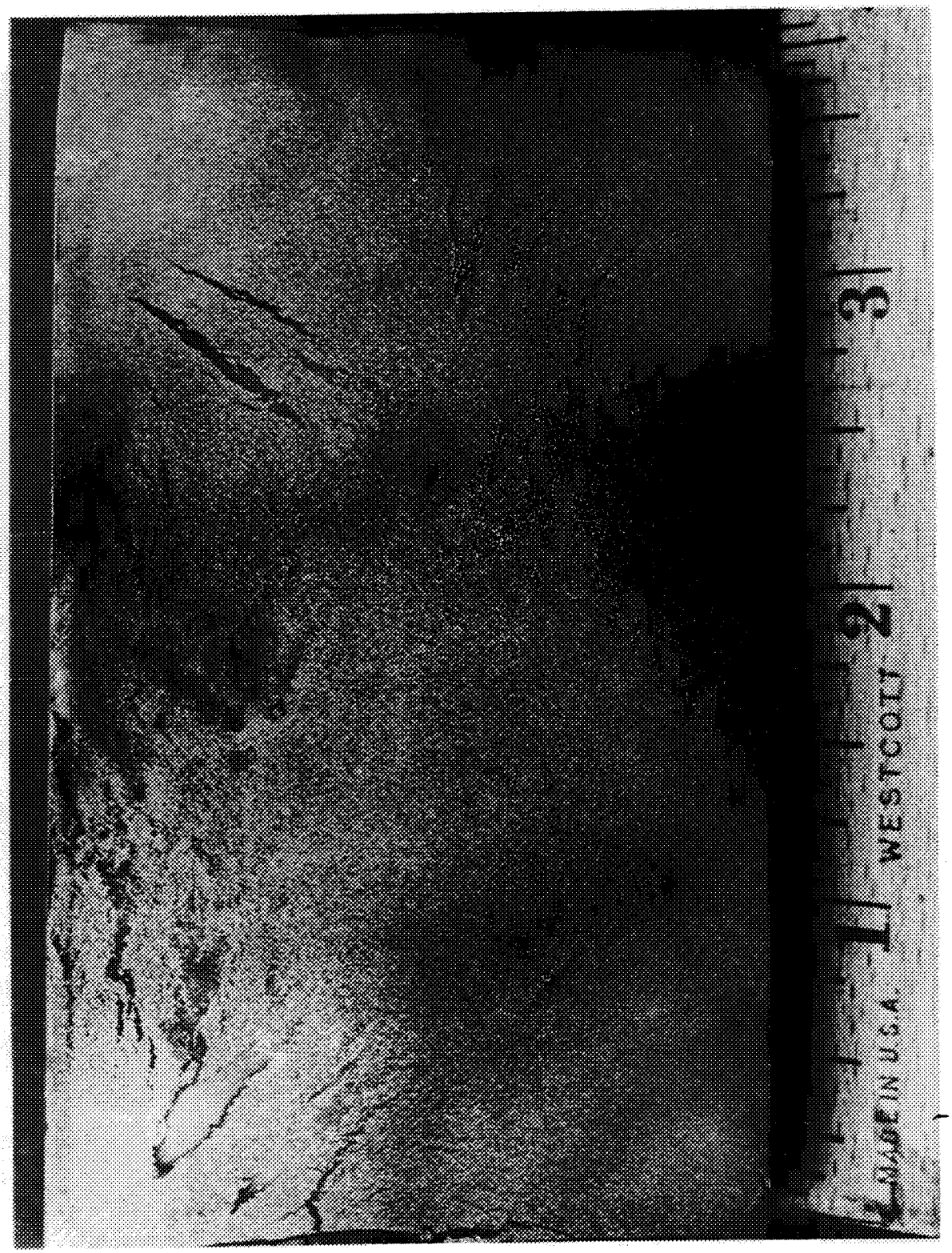

Magnification × 2.1

Etchant: Kallings reagent No. 2

Figure 7. As-squeeze cast macrostructure of billet 4.

Magnification × 2.3 Etchant: Kallings reagent No. 2

Figure 8. As-squeeze cast macrostructure of billet 5.

Magnification × 2.5 Etchant: Kallings reagent No. 2

Figure 9. As-squeeze cast macrostructure of billet 6.

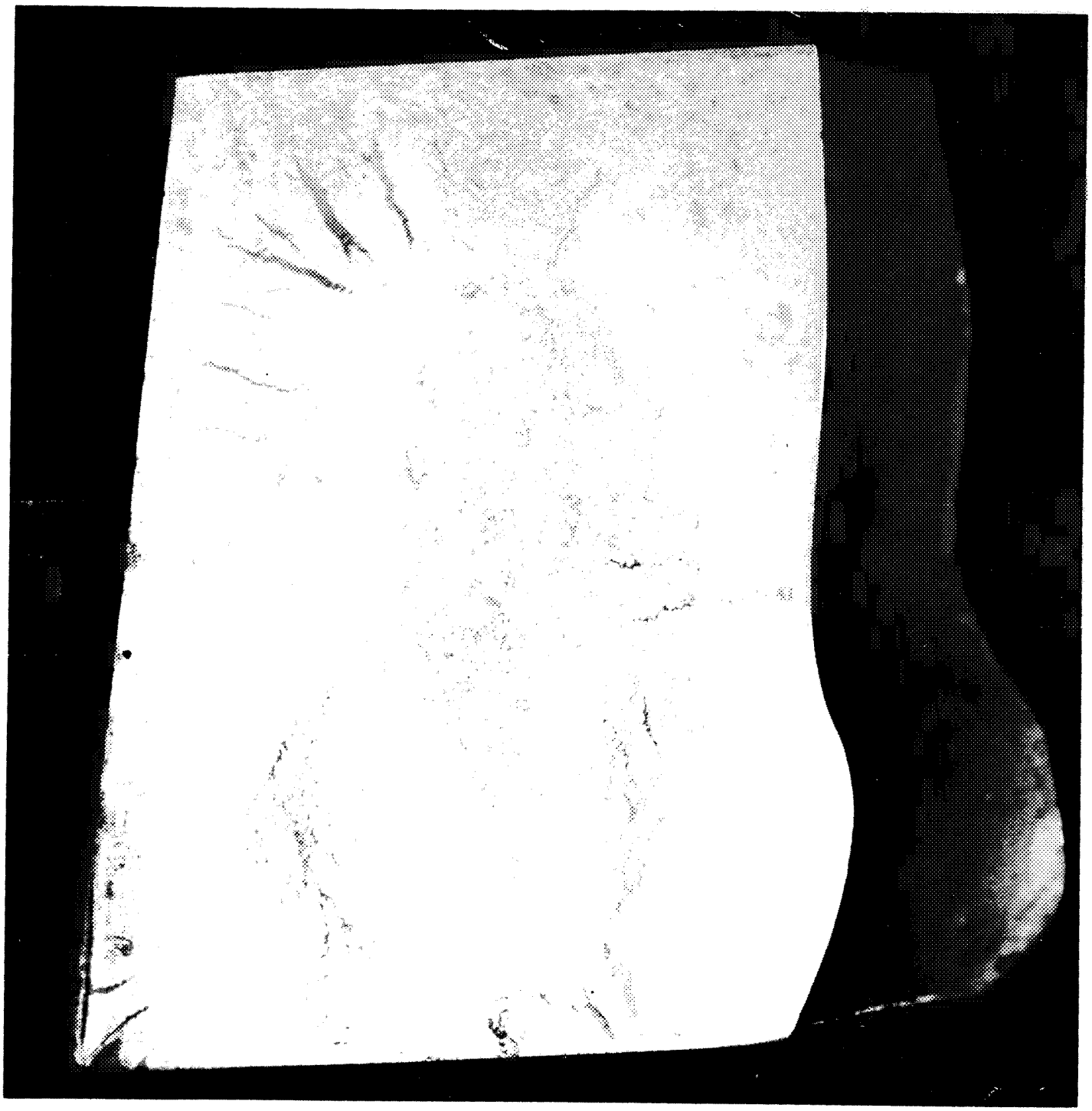

Magnification × 2.3 Etchant: Kallings reagent No. 2

Figure 10. As-squeeze cast macrostructure of billet 9.

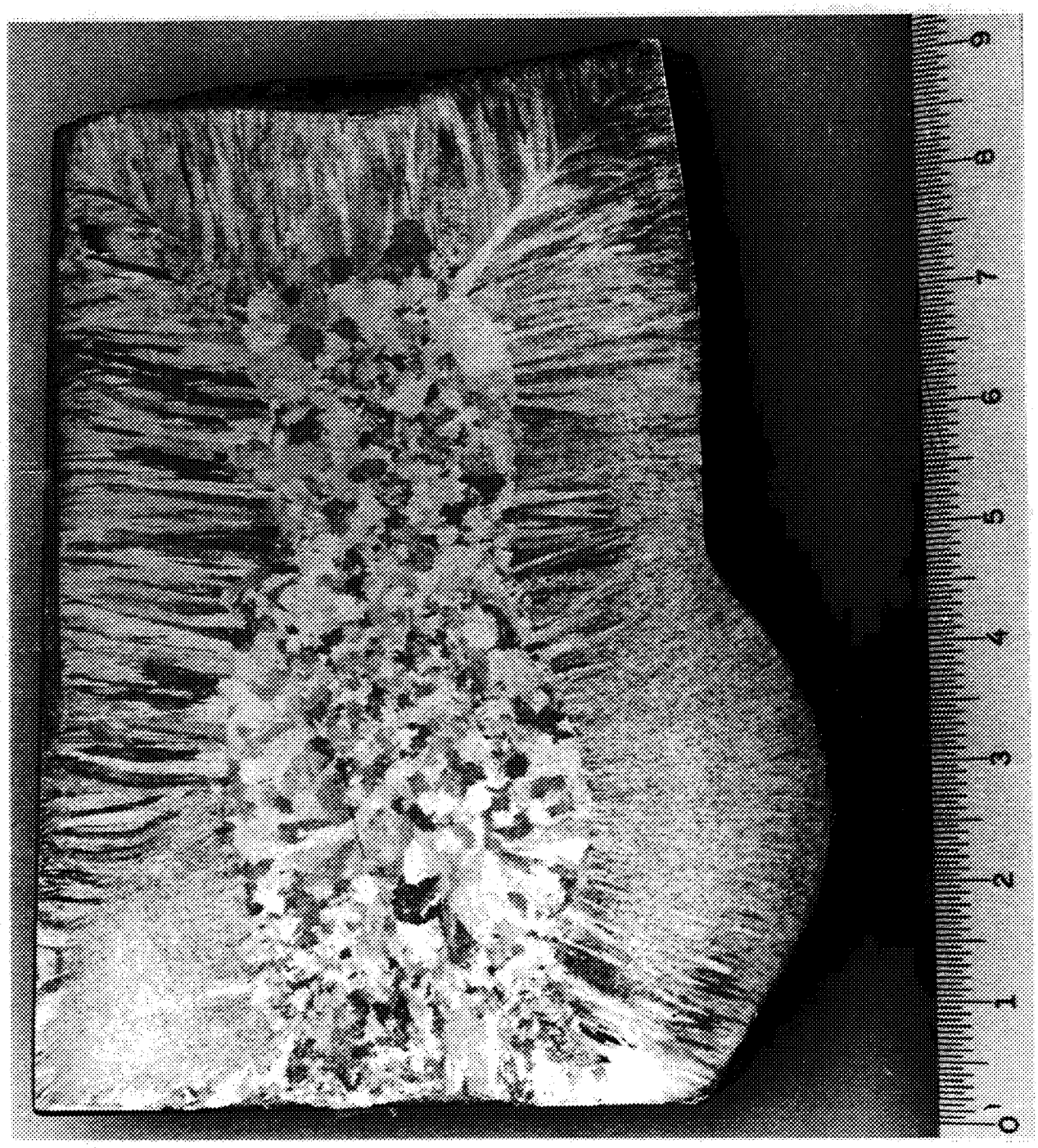

Magnification × 2.2 Etchant: Kallings reagent No. 2

Figure 11. As-squeeze cast macrostructure of billet 12.

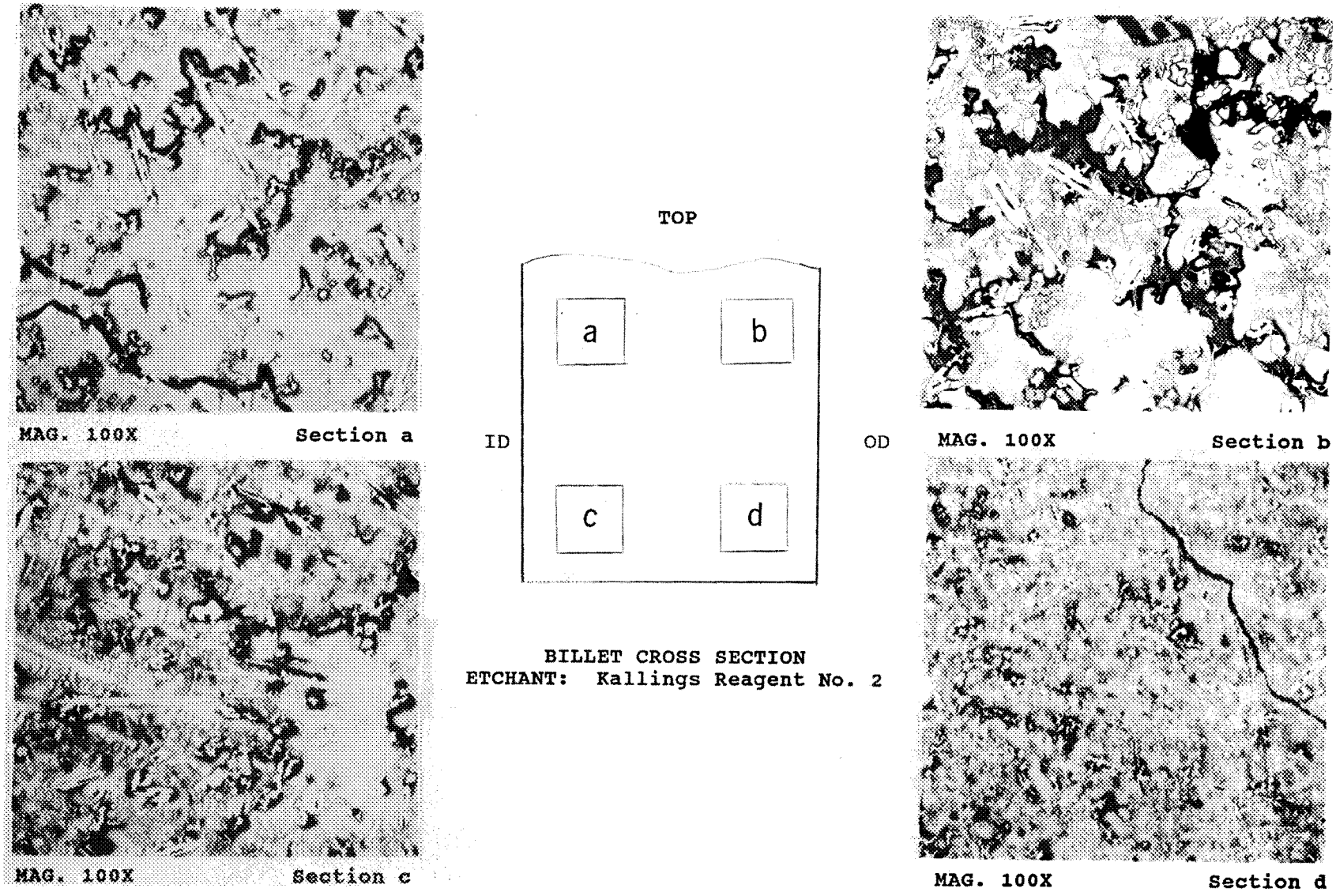

Figure 12. As-squeeze cast microstructures of billet 1.

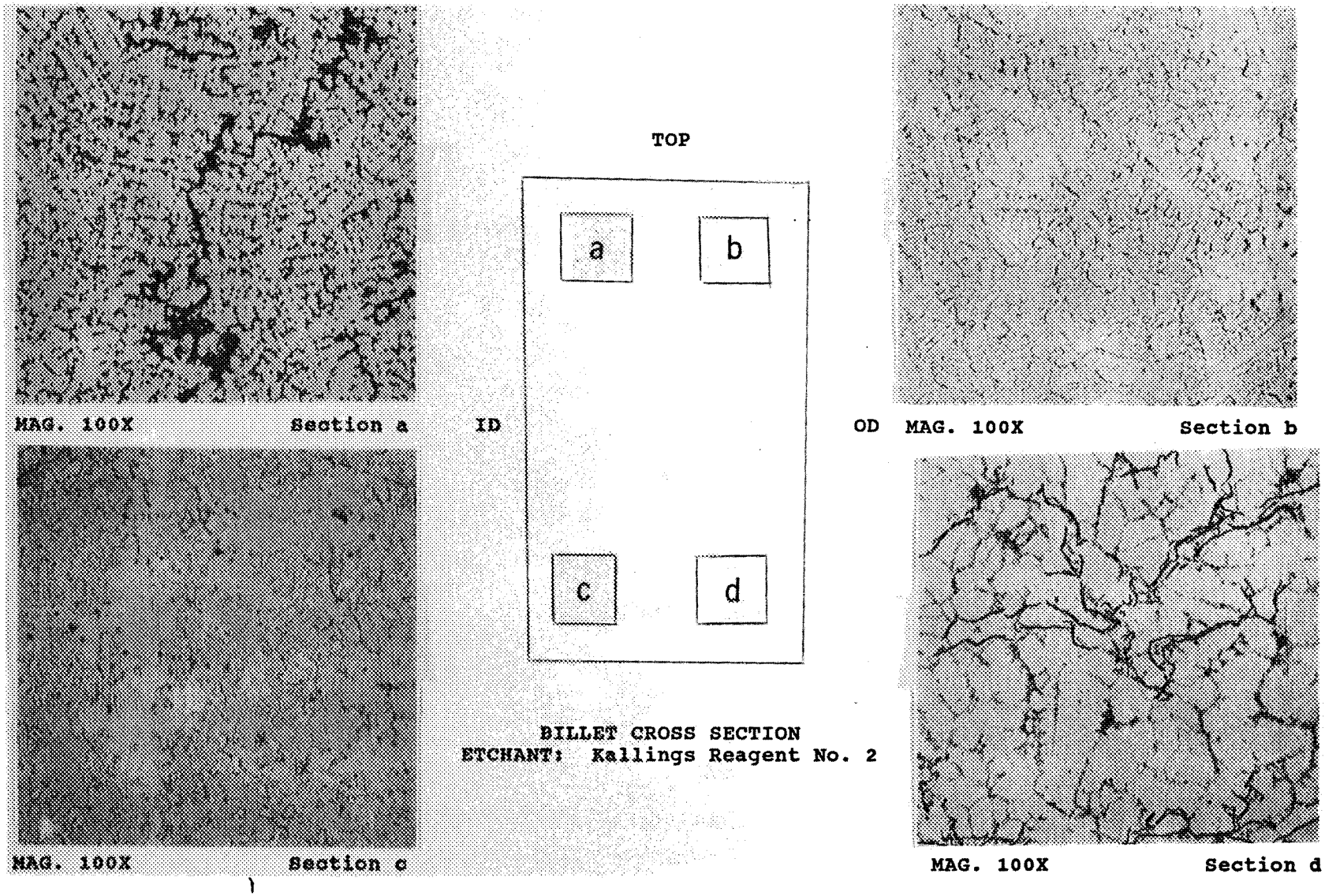

Figure 13. As-squeeze cast microstructures of billet 4.

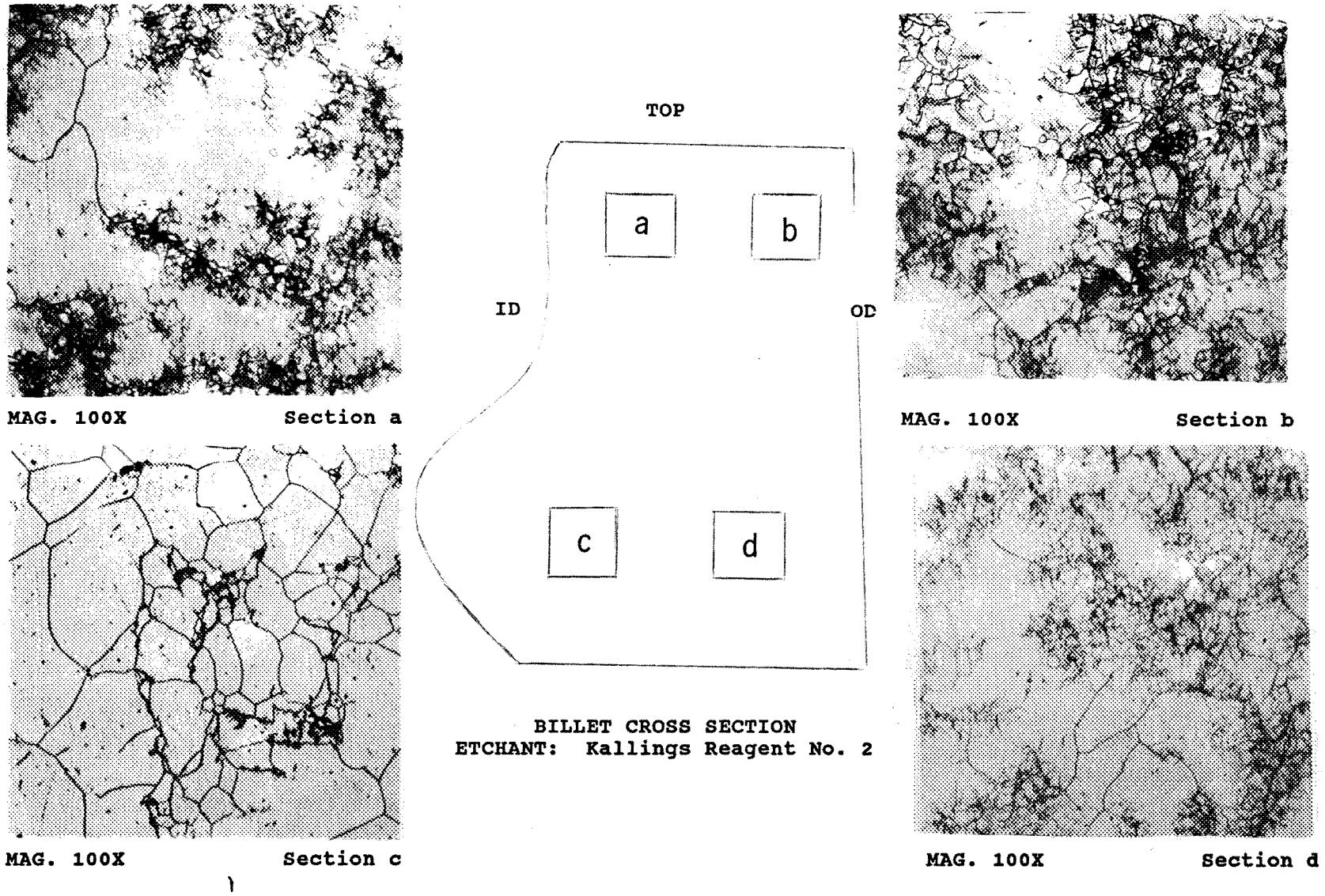

Figure 14. As-squeeze cast microstructures of billet 5.

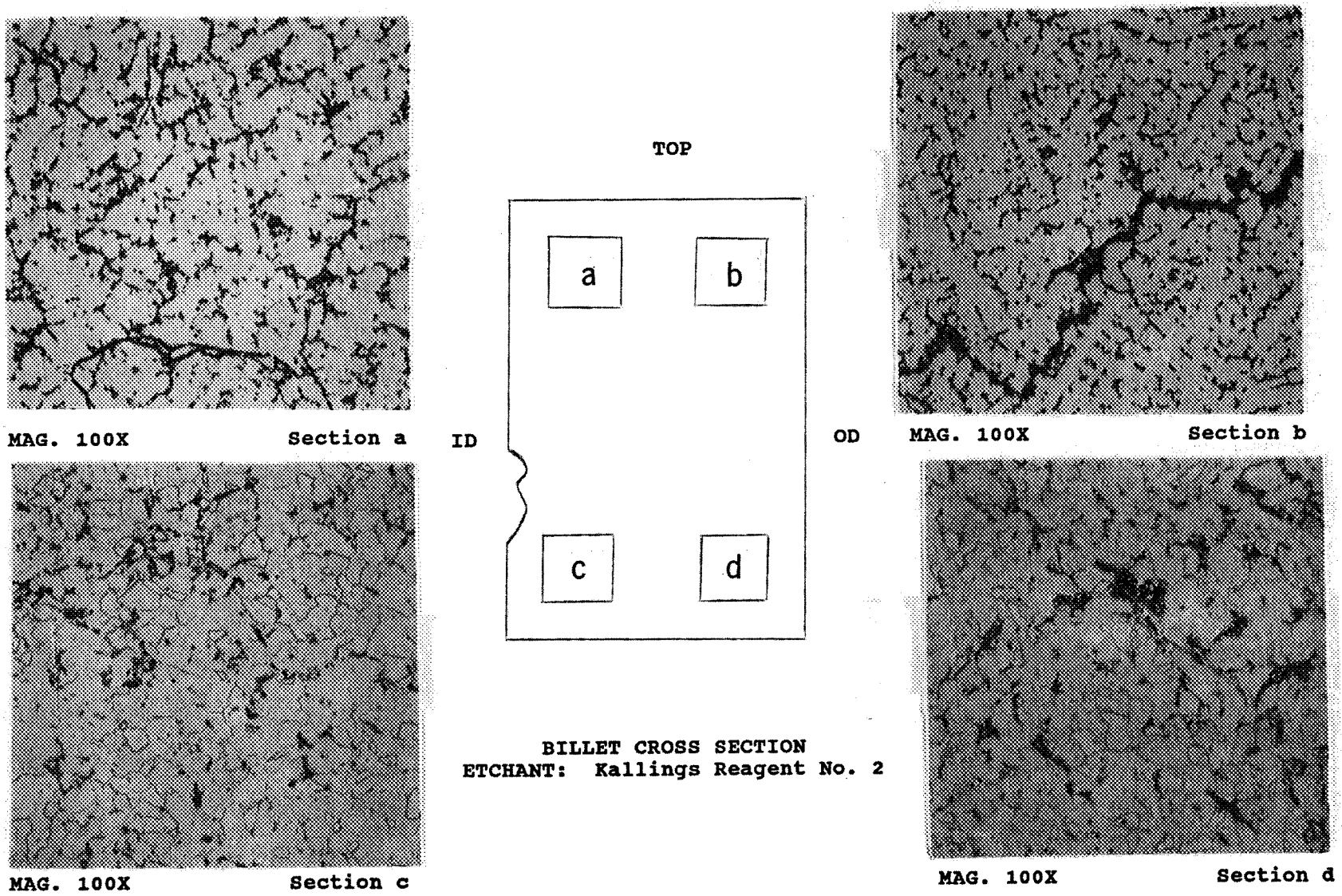

Figure 15. As-squeeze cast microstructures of billet 6.

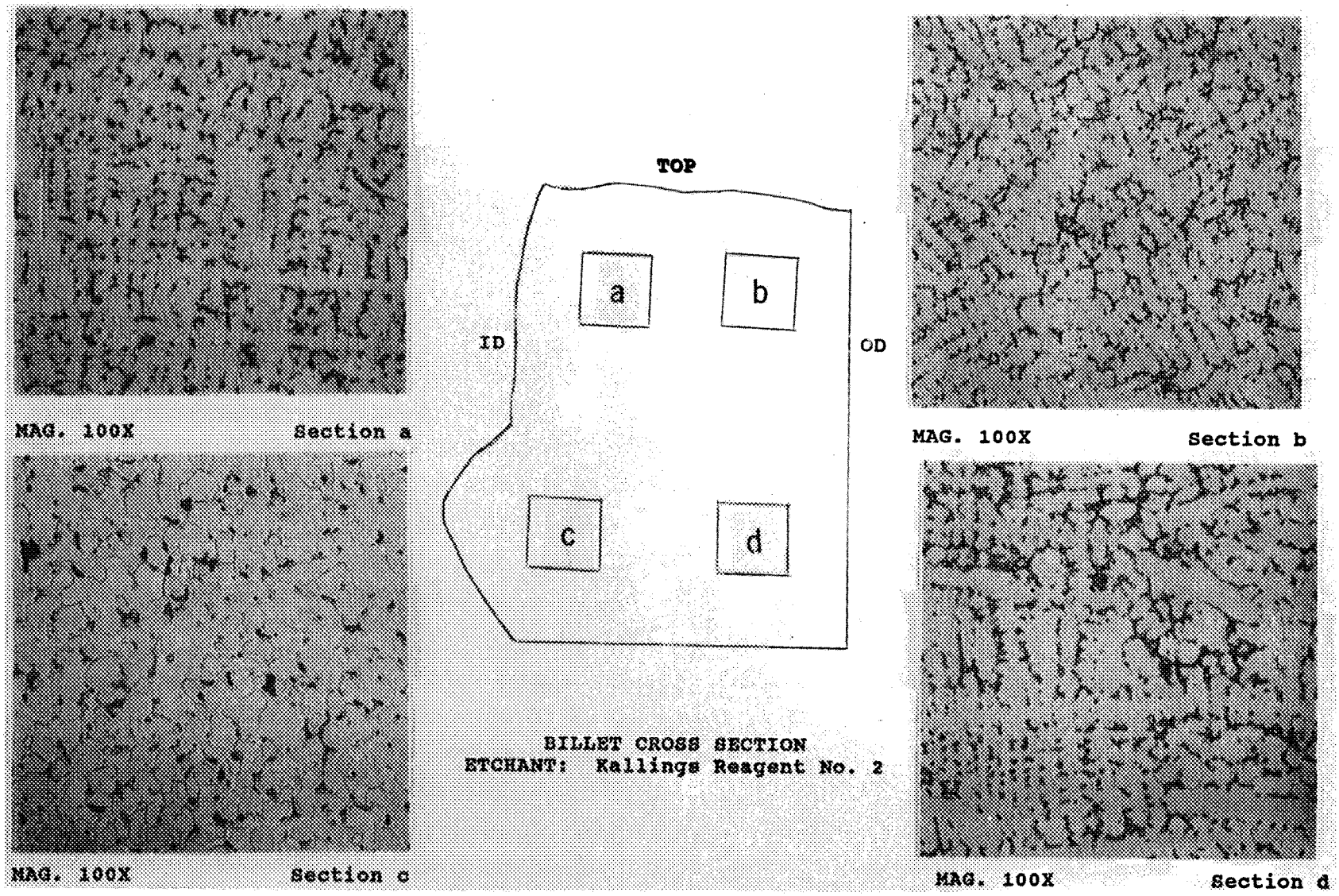

Figure 16. As-squeeze cast microstructures of billet 12.

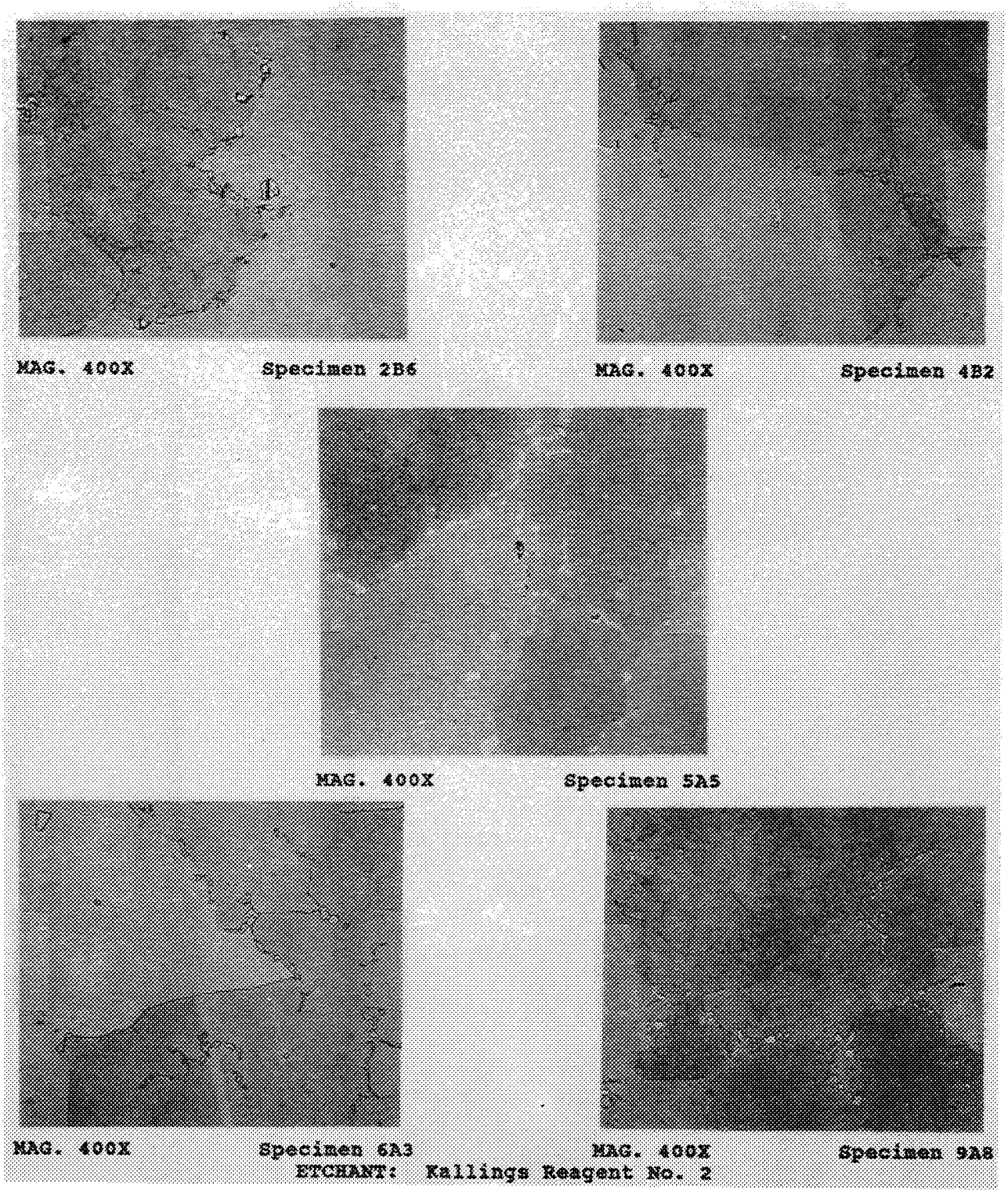

Figure 17. Microstructures characteristic of heat-treated specimens from billets 2, 4, 5, 6, and 9.

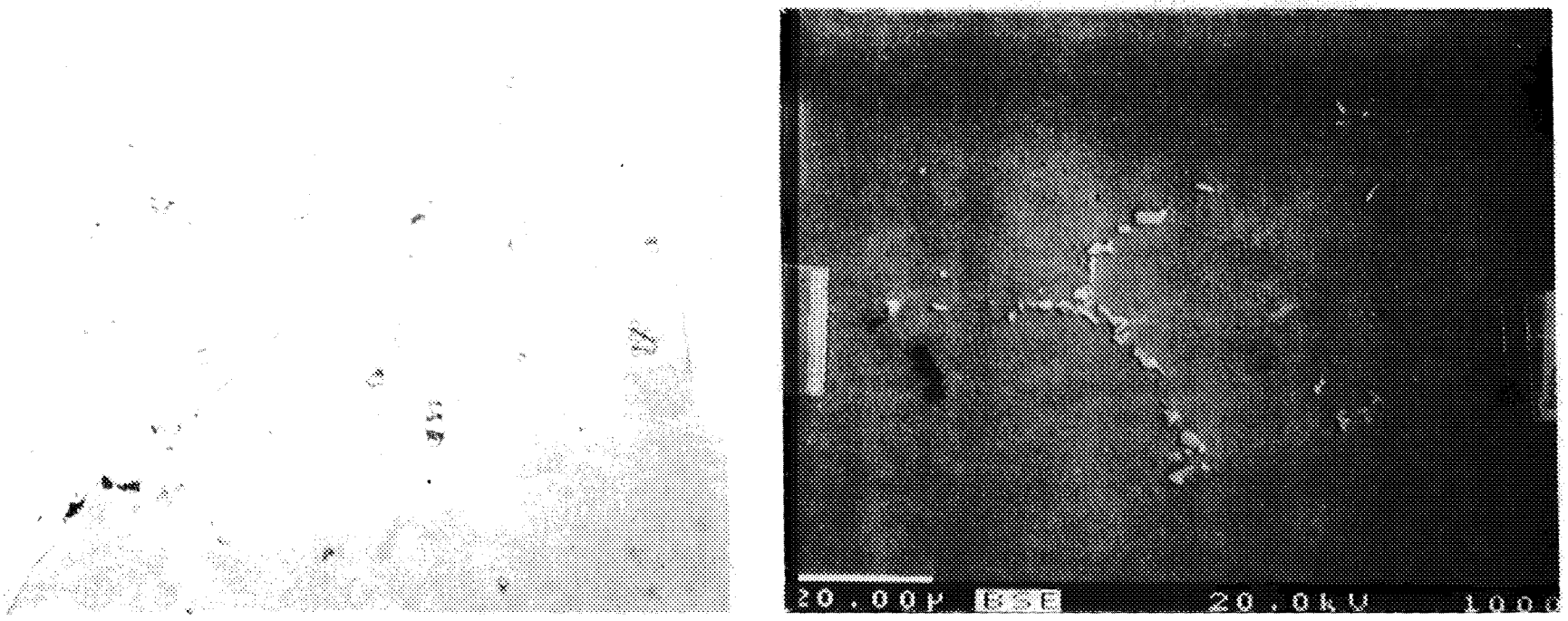

MAG. 400X

MAG. 1000X

ETCHANT: Kallings Reagent No. 2

Figure 18. Microstructures characteristic of heat-treated specimens from billet 12.

APPENDIX

This appendix contains tables of mechanical properties for billets 2, 4, 5, 6, and 9; figures of mechanically tested billet tensile specimen groups, and fracture surfaces representative of billet tensile specimens.

Table A1. Mechanical properties for billets 2A and 2B.

Billet 2A
Longitudinal Tensile Specimens

Specimen Number	Specimen ID	Orientation	Ftu (ksi)	Fty (ksi)	Percent Elongation	Percent RA	Notes
1	2A1	L	151.70	146.10	0.30	1.60	2,4,5,6
2	2A2	L	159.30	136.50	4.30	10.80	3,5,6
3	2A3	L	169.60	150.80	1.70	3.20	1,4,5,6
4	2A4	L	161.20	140.90	4.60	11.60	4,5,6
5	2A5	L	172.80	151.30	6.20	13.10	4,5,6
6	2A6	L	77.60	—	2.00	0.80	4,5,6
7	2A7	L	168.60	145.80	6.30	11.70	3,5,6
8	2A8	L	163.70	145.60	1.00	11.10	2,4,5,6
9	2A9	L	131.40	—	0.20	1.60	2,4,5,6
10	2A10	L	161.00	139.60	5.60	16.90	4,5,6
11	2A11	L	175.00	147.30	11.00	18.30	1,3
12	2A12	L	166.30	143.60	7.80	13.20	4,5,6

Billet 2B
Longitudinal Tensile Specimens

Specimen Number	Specimen ID	Orientation	Ftu (ksi)	Fty (ksi)	Percent Elongation	Percent RA	Notes
1	2B1	L	126.30	—	0.80	0.80	2,4,5,6
2	2B2	L	117.60	—	0.40	5.50	2,4,5,6
3	2B3	L	117.40	—	0.30	1.60	2,4,5,6
4	2B4	L	157.90	141.10	3.80	18.00	3,5,6
5	2B5	L	157.80	138.90	5.90	8.00	4,5,6
6	2B6	L	166.50	143.30	7.90	7.00	4
7	2B7	L	79.00	—	0.10	0.00	2,4,5,6
8	2B8	L	137.50	135.30	0.00	7.80	4,5,6
9	2B9	L	123.40	—	1.80	5.50	4,5,6
10	2B10	L	85.80	—	0.00	3.10	1,4,5,6
11	2B11	L	100.60	—	0.00	1.60	1,4,5,6
12	2B12	L	113.30	—	0.60	2.40	2,4,5,6

Notes:
1. Broke at gauge mark
2. Broke outside gauge marks
3. 45° shear plane type fracture
4. Semiflat fracture surface
5. Intermittent gold discoloration
6. Crack-like features perpendicular to fracture surface
7. Shrinkage areas
8. Dendrites associated with shrinkage areas
9. Unable to determine yield strength

Ftu Ultimate tensile strength
Fty Yield strength
A. Homogenization treatment A
B. Homogenization treatment B

Table A2. Mechanical properties for billets 4A and 4B.

Billet 4A
Longitudinal Tensile Specimens

Specimen Number	Specimen ID	Orientation	Ftu (ksi)	Fty (ksi)	Percent Elongation	Percent RA	Notes
1	4A1	L	86.2	—	0.2	1.6	2,3,5,7,8
2	4A2	L	157.8	146.7	2.9	8.6	4,5,6
3	4A3	L	165.2	147.2	5.1	7.1	3,5,6
4	4A4	L	130.2	—	0.1	0.0	2,4,5,6,7,8
5	4A5	L	149.5	145.8	0.7	4.0	1,3,5,6
6	4A6	L	158.1	145.8	0.3	6.3	2,3,5,6
7	4A7	L	142.6	140.3	0.5	4.7	2,4,5,6,7
8	4A8	L	157.3	145.3	2.3	7.9	3,5,6
9	4A9	L	158.9	147.3	2.4	7.1	4,5,6
10	4A10	L	150.1	142.1	2.0	6.3	3,5,6
11	4A11	L	162.4	147.5	3.1	7.8	3,5,6
12	4A12	L	165.2	151.8	3.2	7.8	3,5,6

Billet 4B
Longitudinal Tensile Specimens

Specimen Number	Specimen ID	Orientation	Ftu (ksi)	Fty (ksi)	Percent Elongation	Percent RA	Notes
1	4B1	L	84.3	—	1.6	0.0	1,3,5,7
2	4B2	L	163.2	143.7	3.2	7.9	3,5,6
3	4B3	L	155.5	148.7	0.3	7.8	2,4,5,6
4	4B4	L	140.8	135.5	2.5	7.1	3,5,6
5	4B6	L	167.0	150.4	3.1	9.4	3,5,6
6	4B7	L	147.9	139.6	3.3	7.9	3,5
7	4B8	L	127.1	—	1.9	2.4	3,5,6,7,8
8	4B9	L	161.5	149.3	3.1	10.1	3,5,6
9	4B10	L	125.8	—	1.7	0.8	3,7
10	4B11	L	174.9	144.7	0.5	4.8	3,5,6
11	4B12	L	147.4	132.2	3.8	11.6	3,5,6

Notes:
1. Broke at gauge mark
2. Broke outside gauge marks
3. 45° shear plane type fracture
4. Semiflat fracture surface
5. Intermittent gold discoloration
6. Crack-like features perpendicular to fracture surface
7. Shrinkage areas
8. Dendrites associated with shrinkage areas
9. Unable to determine yield strength

Ftu Ultimate tensile strength
Fty Yield strength
A. Homogenization treatment A
B. Homogenization treatment B

Table A3. Mechanical properties for billets 5A and 5B.

Billet 5A
Longitudinal Tensile Specimens

Specimen Number	Specimen ID	Orientation	Ftu (ksi)	Fty (ksi)	Percent Elongation	Percent RA	Notes
1	5A2	L	137.40	130.30	1.80	5.50	3,5,6
2	5A3	L	149.90	138.40	2.10	7.10	1,3,5,6
3	5A4	L	153.20	143.80	1.20	2.40	1.4,5,6
4	5A5	L	159.70	141.60	2.00	6.30	3,5,6
5	5A6	L	151.90	142.40	1.10	3.20	1,3,5
6	5A7	L	132.10	127.50	1.90	3.20	3,5,6
7	5A8	L	149.00	137.00	0.60	3.20	1,4,5,6
8	5A9	L	143.50	137.20	1.50	4.00	4,5,6
9	5A10	L	161.40	144.80	1.20	2.40	2,4,5,6
10	5A12	L	153.30	140.20	1.50	7.80	4,5,6
11	5A13	L	157.10	143.80	1.60	6.30	4,5,6

Billet 5B
Longitudinal Tensile Specimens

Specimen Number	Specimen ID	Orientation	Ftu (ksi)	Fty (ksi)	Percent Elongation	Percent RA	Notes
1	5B1	L	153.40	140.30	2.00	7.51	4,5,6
2	5B2	L	146.70	138.70	2.00	10.14	1,4,5,6
3	5B3	L	136.90	121.80	4.00	6.62	1,4,5,6
4	5B4	L	151.40	138.10	1.60	7.02	4,5,6
5	5B7	L	129.10	119.70	0.20	5.88	1,4,5,6
6	5B8	L	158.30	143.40	1.70	5.08	1,4,5,6
7	5B9	L	145.70	135.70	2.50	6.26	4,5,6
8	5B10	L	149.50	138.30	2.00	2.57	1,3,5,6
9	5B11	L	148.20	139.30	3.00	7.97	4,5,6
10	5B12	L	145.70	143.00	0.50	—	2,4,5,6

Notes:
1. Broke at gauge mark
2. Broke outside gauge marks
3. 45° shear plane type fracture
4. Semiflat fracture surface
5. Intermittent gold discoloration
6. Crack-like features perpendicular to fracture surface
7. Shrinkage areas
8. Dendrites associated with shrinkage areas
9. Unable to determine yield strength

Ftu Ultimate tensile strength
Fty Yield strength
A. Homogenization treatment A
B. Homogenization treatment B

Table A4. Mechanical Properties for billets 6A and 6B.

Billet 6A
Longitudinal Tensile Specimens

Specimen Number	Specimen ID	Orientation	Ftu (ksi)	Fty (ksi)	Percent Elongation	Percent RA	Notes
1	6A1	L	164.1	151.6	3.2	7.1	3,5,6
2	6A3	L	163.0	149.6	3.9	8.6	3,5,6
3	6A4	L	166.8	149.9	3.8	9.4	3,5,6
4	6A6	L	165.9	151.0	3.7	8.6	3,5,6
5	6A7	L	145.8	140.6	2.4	4.0	3,5,6
6	6A9	L	150.4	147.6	1.7	7.8	3,5,6
7	6A10	L	121.7	—	0.2	3.7	2,3,5,6
8	6A12	L	170.1	153.3	3.6	8.6	3,5,6

Billet 6B
Longitudinal Tensile Specimens

Specimen Number	Specimen ID	Orientation	Ftu (ksi)	Fty (ksi)	Percent Elongation	Percent RA	Notes
1	6B1	L	111.2	—	0.0	0.0	
2	6B3	L	153.8	144.7	2.4	7.1	3,5,6
3	6B4	L	163.8	146.0	3.8	7.1	3,5,6
4	6B6	L	131.6	128.1	2.1	7.9	3,5,6
5	6B7	L	146.3	142.4	1.8	7.9	3,5,6
6	6B8	L	148.7	144.3	2.1	5.5	3,5,6
7	6B9	L	160.9	152.5	2.4	10.9	3,5,6
8	6B11	L	111.0	110.3	1.8	2.4	3,5,6
9	6B12	L	160.0	152.1	0.5	1.6	2,3,5,6

Notes:
1. Broke at gauge mark
2. Broke outside gauge marks
3. 45° shear plane type fracture
4. Semiflat fracture surface
5. Intermittent gold discoloration
6. Crack-like features perpendicular to fracture surface
7. Shrinkage areas
8. Dendrites associated with shrinkage areas
9. Unable to determine yield strength

Ftu Ultimate tensile strength
Fty Yield strength
A. Homogenization treatment A
B. Homogenization treatment B

Table A5. Mechanical properties for billet 9A.

Billet 9A
Longitudinal Tensile Specimens

Specimen Number	Specimen ID	Orientation	Ftu (ksi)	Fty (ksi)	Percent Elongation	Percent RA	Notes
1	9-1	L	130.5	116.3	3.4	6.2	4,5,6,7
2	9-2	L	125.8	116.8	2.3	3.9	3,5,6
3	9-3	L	113.4	111.2	2.4	0.8	3,5,6
4	9-4	L	134.1	120.0	3.2	8.7	3,5,6,7
5	9-5	L	129.8	115.4	3.9	3.9	4,5,6
6	9-6	L	138.8	122.1	1.7	3.9	2,4,5,6
7	9-7	L	131.2	116.1	3.0	4.7	4,5,6
8	9-8	L	144.9	119.8	5.8	6.3	1,4,5,6
9	9-9	L	137.6	123.5	4.2	65.7	4,5,6
10	9-10	L	140.8	122.7	5.7	15.4	4,5,6
11	9-11	L	118.0	113.1	2.3	2.4	4,5,6
12	9-12	L	86.2	—	1.4	0.8	4,5,6,7

Notes:
1. Broke at gauge mark
2. Broke outside gauge marks
3. 45° shear plane type fracture
4. Semiflat fracture surface
5. Intermittent gold discoloration
6. Crack-like features perpendicular to fracture surface
7. Shrinkage areas
8. Dendrites associated with shrinkage areas
9. Unable to determine yield strength

Ftu Ultimate tensile strength
Fty Yield strength
A. Homogenization treatment A

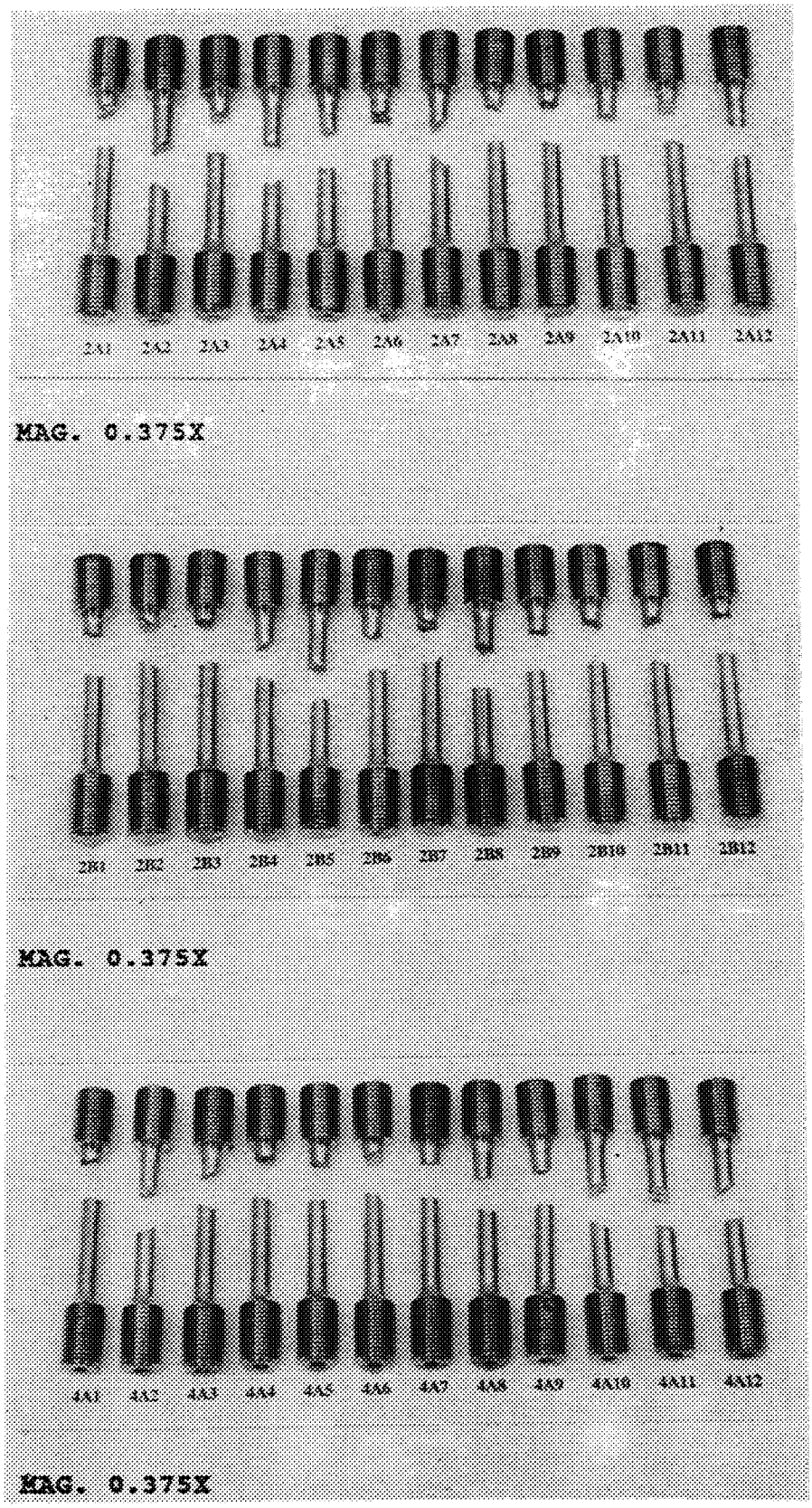

Figure A1. Mechanically tested tensile specimen groups 2A, 2B, and 4A.

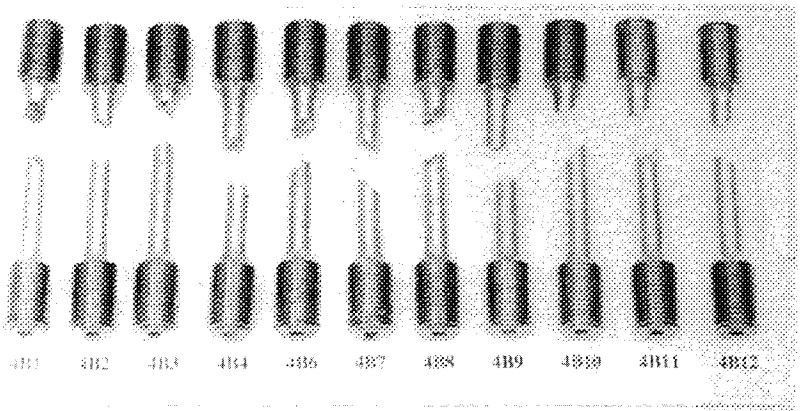

MAG. 0.375X

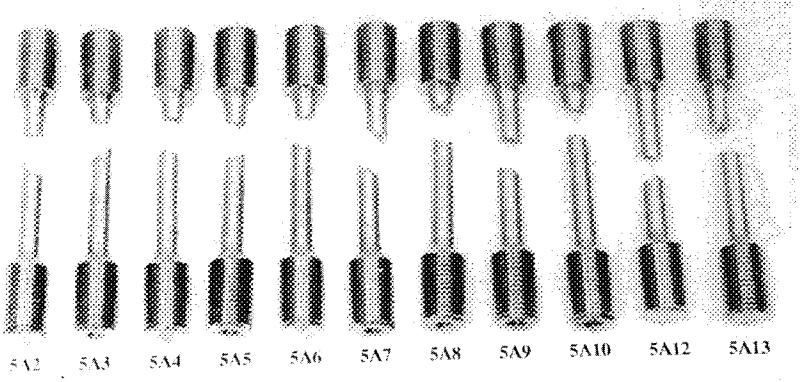

MAG. 0.375X

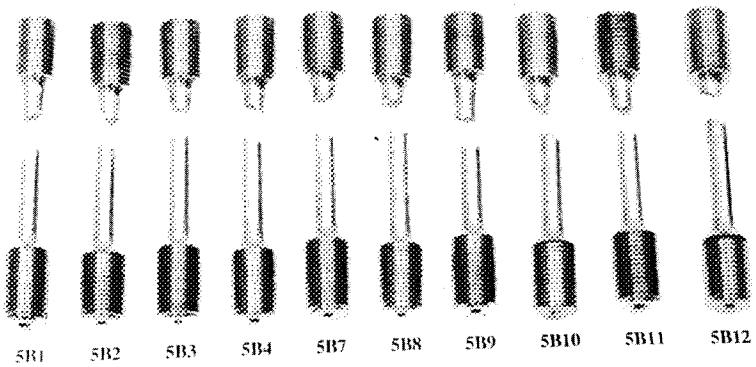

MAG. 0.375X

Figure A2. Mechanically tested tensile specimens groups 4B, 5A, and 5B.

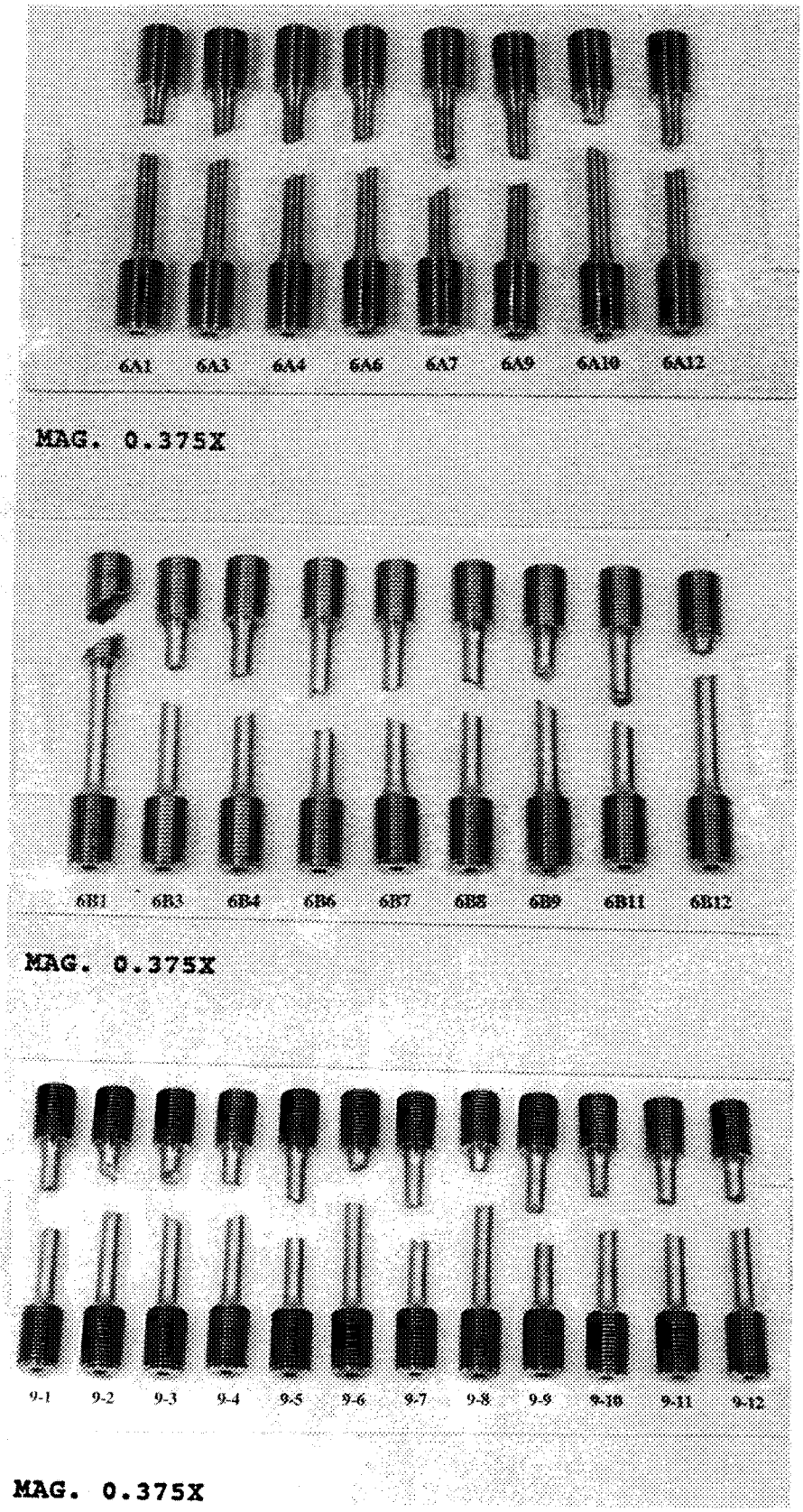

Figure A3. Mechanically tested tensile specimen groups 6A, 6B, and 9A.

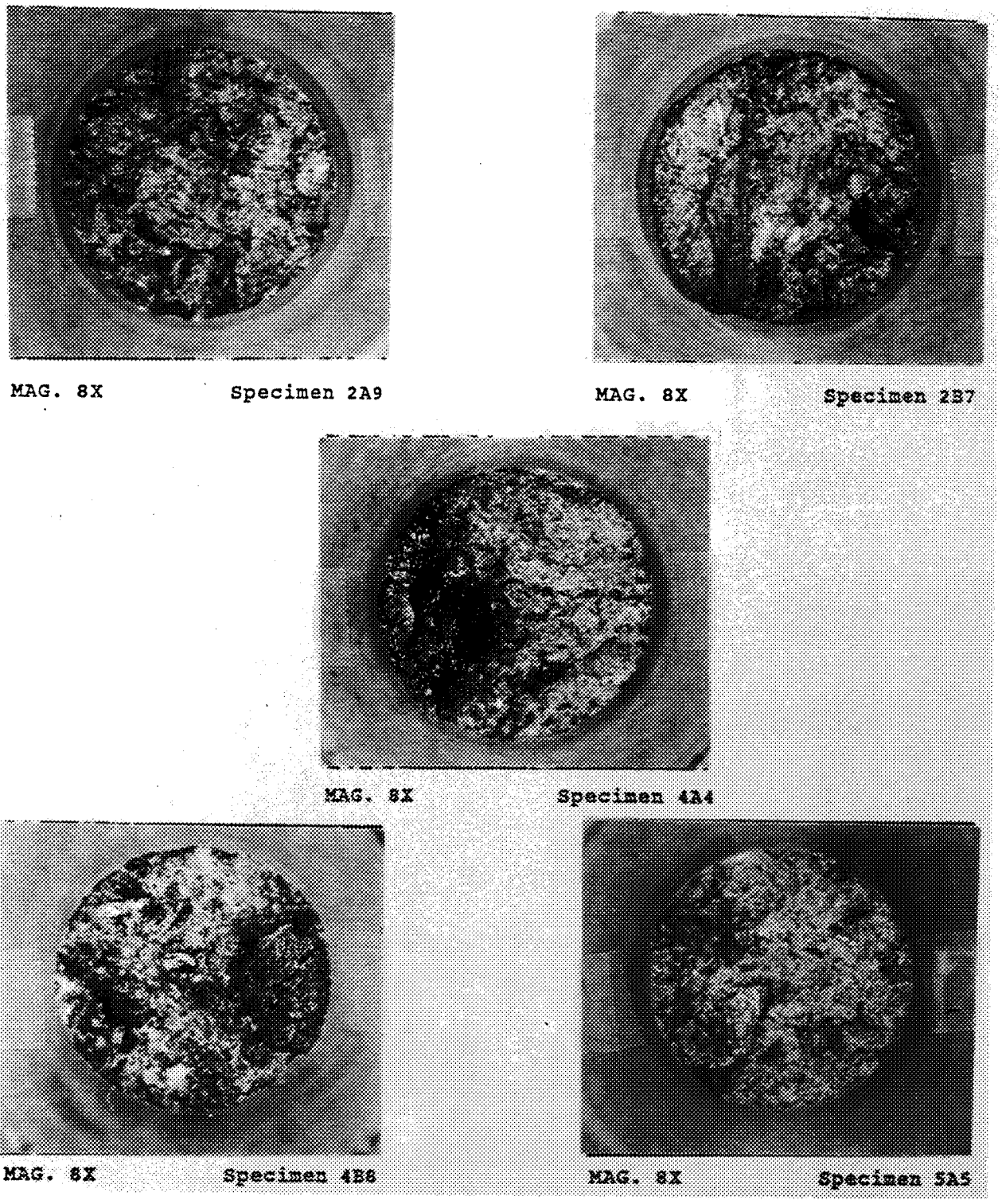

Figure A4. Fracture surfaces representative of billet tensile specimens.

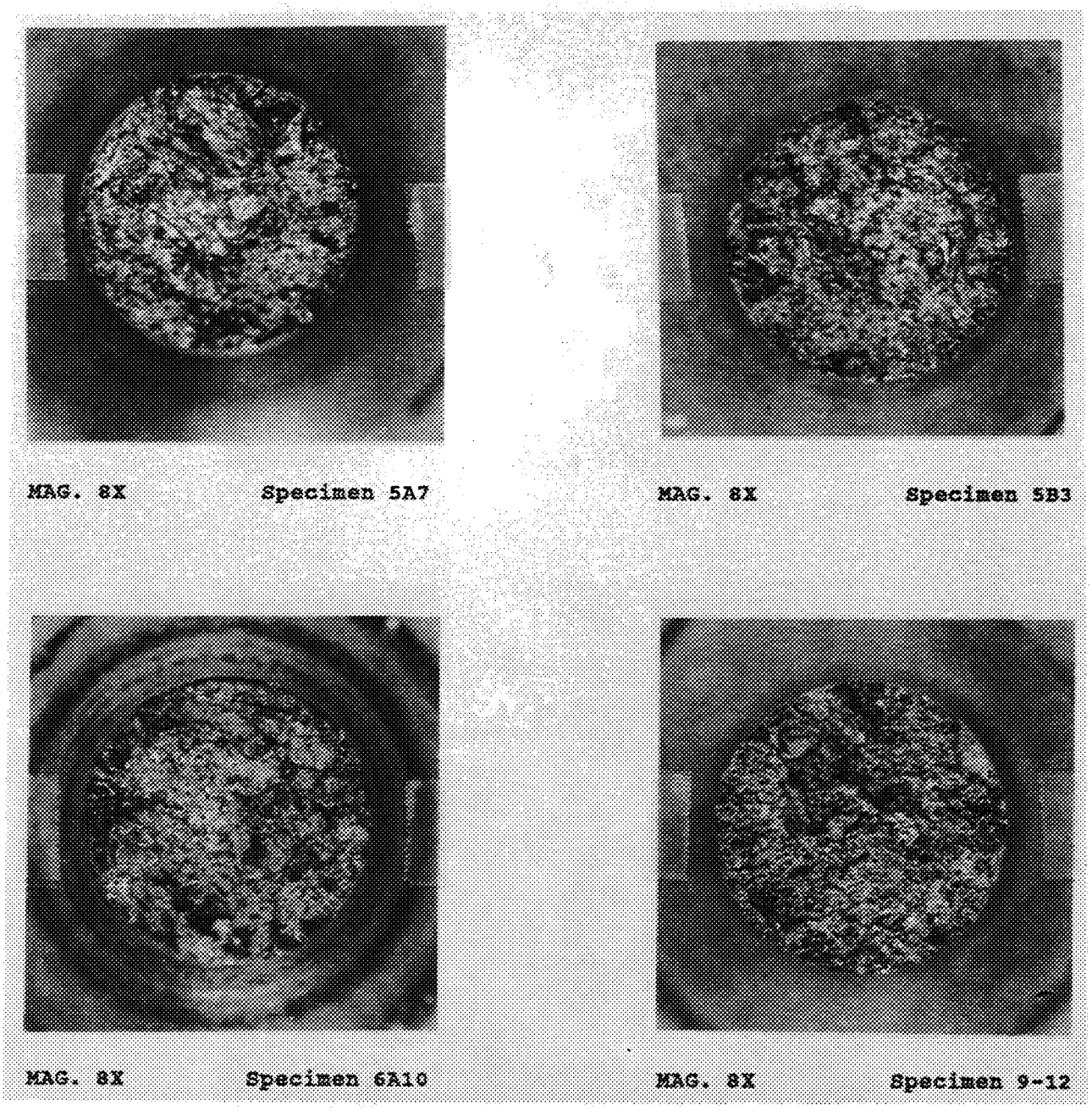

Figure A5. Fracture surfaces representative of billet tensile specimens.

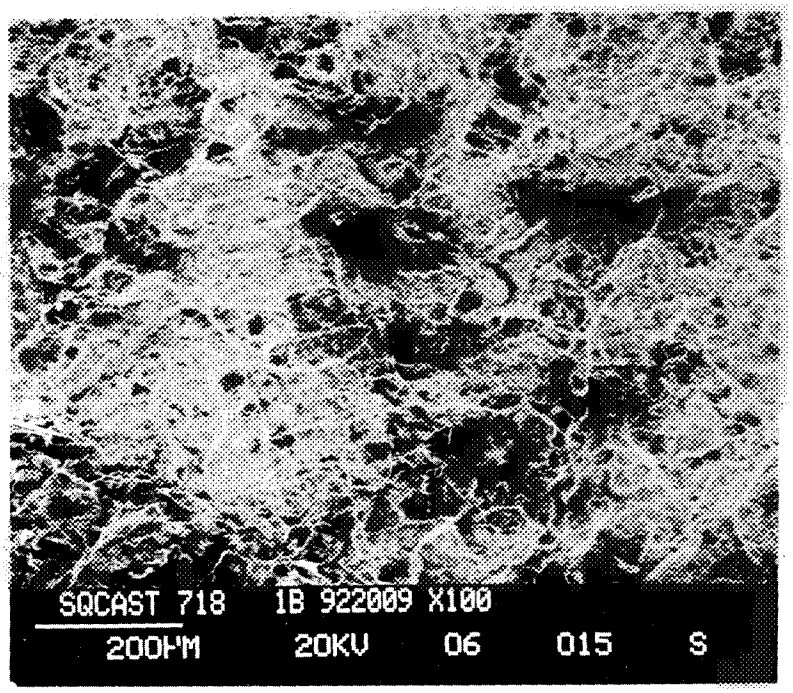

MAG. 100X

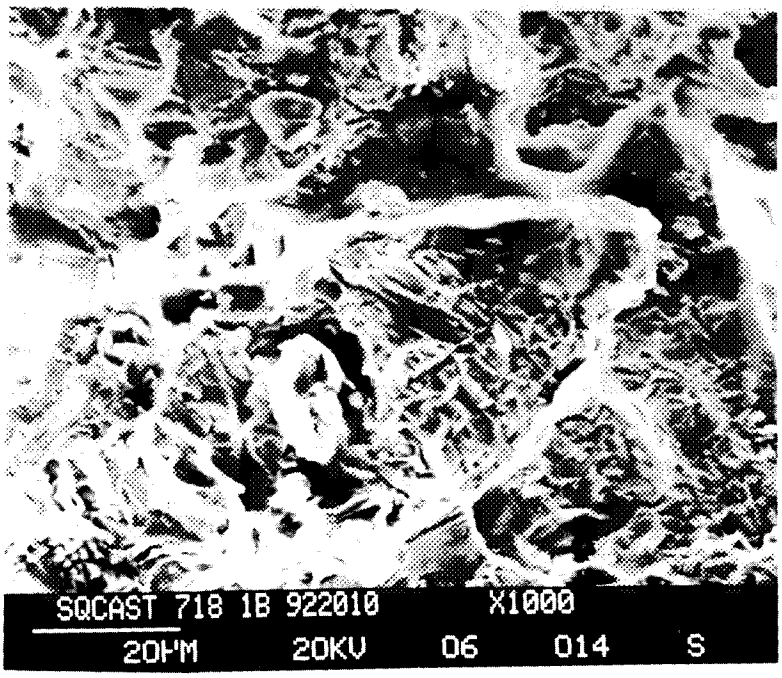

MAG. 1000X

Figure A6. SEM fractographs from billet 12 tensile test specimens.

APPROVAL

AN INVESTIGATION OF SQUEEZE-CAST ALLOY 718

By W.R. Gamwell

The information in this report has been reviewed for technical content. Review of any information concerning Department of Defense or nuclear energy activities or programs has been made by the MSFC Security Classification Officer. This report, in its entirety, has been determined to be unclassified.

Biligan N. Bhat

B.N. BHAT
Chief, Metallurgy Research Branch

Paul M. Munafo

P.M. MUNAFO
Chief, Metallic Materials Division

Paul H. Schuerer

P.H. SCHUERER
Director, Materials and Processes Laboratory

☆ U.S. GOVERNMENT PRINTING OFFICE 1993—733-050/80089

REPORT DOCUMENTATION PAGE

Form Approved
OMB No. 0704-0188

1. AGENCY USE ONLY *(Leave blank)*	2. REPORT DATE	3. REPORT TYPE AND DATES COVERED
	June 1993	Technical Memorandum

4. TITLE AND SUBTITLE

An Investigation of Squeeze-Cast Alloy 718
(CDDF Final Report No. 90-10)

5. FUNDING NUMBERS

6. AUTHOR(S)

W.R. Gamwell

7. PERFORMING ORGANIZATION NAME(S) AND ADDRESS(ES)

George C. Marshall Space Flight Center
Marshall Space Flight Center, Alabama 35812

8. PERFORMING ORGANIZATION REPORT NUMBER

9. SPONSORING/MONITORING AGENCY NAME(S) AND ADDRESS(ES)

National Aeronautics and Space Administration
Washington, DC 20546

10. SPONSORING/MONITORING AGENCY REPORT NUMBER

NASA TM - 108412

11. SUPPLEMENTARY NOTES

Prepared by Materials and Processes Laboratory, Science and Engineering Directorate.

12a. DISTRIBUTION/AVAILABILITY STATEMENT

Unclassified—Unlimited

12b. DISTRIBUTION CODE

13. ABSTRACT *(Maximum 200 words)*

Alloy 718 billets produced by the squeeze-cast process have been evaluated for use as potential replacements for propulsion engine components which are normally produced from forgings. Alloy 718 billets were produced using various processing conditions. Structural characterizations were performed on "as-cast" billets. As-cast billets were then homogenized and solution treated and aged according to conventional heat-treatment practices for this alloy. Mechanical property evaluations were performed on heat-treated billets.

As-cast macrostructures and microstructures varied with squeeze-cast processing parameters. Mechanical properties varied with squeeze-cast processing parameters and heat treatments. One billet exhibited a defect free, refined microstructure, with mechanical properties approaching those of wrought alloy 718 bar, confirming the feasibility of squeeze-casting alloy 718. However, further process optimization is required, and further structural and mechanical property improvements are expected with process optimization.

14. SUBJECT TERMS	15. NUMBER OF PAGES
squeeze casting, alloy 718, mechanical properties, structural characteristics	50
	16. PRICE CODE NTIS

17. SECURITY CLASSIFICATION OF REPORT	18. SECURITY CLASSIFICATION OF THIS PAGE	19. SECURITY CLASSIFICATION OF ABSTRACT	20. LIMITATION OF ABSTRACT
Unclassified	Unclassified	Unclassified	Unlimited